ANÁLISIS TRANSCRIPTÓMICO GLOBAL DEL SILENCIAMIENTO DE *FUCA1* EN QUERATINOCITOS REVELA NUEVOS HALLAZGOS SOBRE LA PATOGENESIS DE LAS LESIONES CUTÁNEAS DE LA FUCOSIDOSIS

DANYELA FAISURY VALERO RUBIO

UNIVERSIDAD COLEGIO MAYOR DE NUESTRA SEÑORA DEL ROSARIO

ESCUELA DE MEDICINA Y CIENCIAS DE LA SALUD

MAESTRÍA EN GENÉTICA HUMANA

BOGOTÁ, D.C.

MAYO 2018

ANÁLISIS TRANSCRIPTÓMICO GLOBAL DEL SILENCIAMIENTO DE *FUCA1* EN QUERATINOCITOS REVELA NUEVOS HALLAZGOS SOBRE LA PATOGENESIS DE LAS LESIONES CUTÁNEAS DE LA FUCOSIDOSIS

DANYELA FAISURY VALERO RUBIO

TRABAJO DE GRADO

Presentado como requisito parcial para optar al título de

MAGISTER EN GENÉTICA HUMANA

DIRECTOR

PAUL LAISSUE MD., MSc., PhD., HDR

CODIRECTORA

DORA FONSECA Biol., MSc., PhD

UNIVERSIDAD COLEGIO MAYOR DE NUESTRA SEÑORA DEL ROSARIO

ESCUELA DE MEDICINA Y CIENCIAS DE LA SALUD

MAESTRÍA EN GENÉTICA HUMANA

BOGOTÁ, D.C.

MAYO, 2018.

NOTA DE SALVEDAD DE RESPONSABILIDAD INSTITUCIONAL

"La Universidad del Rosario no se hace responsable por los conceptos emitidos por los investigadores en su trabajo, solo velará por el rigor científico, metodológico y ético del mismo en aras de la búsqueda de la verdad y la justicia".

ANÁLISIS TRANSCRIPTÓMICO GLOBAL DEL SILENCIAMIENTO DE *FUCA1* EN QUERATINOCITOS REVELA NUEVOS HALLAZGOS SOBRE LA PATOGENESIS DE LAS LESIONES CUTÁNEAS DE LA FUCOSIDOSIS.

DANYELA FAISURY VALERO RUBIO

APROBADO

_____

PAUL LAISSUE MD, MSc, PhD

DIRECTOR

_____ _____

JURADO **JURADO**

Agradecimientos

A mi familia y a Bernardo, por su amor, su esfuerzo, por creer en mí y apoyarme en todo momento para poder cumplir mis metas.

Al Dr. Paul Laissue, por sus enseñanzas, guía y apoyo durante el desarrollo de este trabajo de investigación.

A la Dra. Dora Fonseca por acompañarme, guiarme, por confiar en mí y brindarme su apoyo a lo largo de la maestría.

A July Buitrago, Carolina sierra, Karen Jimenez y mis compañeros de maestria por brindarme su amistad incondicional, por apoyarme siempre que los necesite.

A todos los integrantes del CIGGUR, por transmitirme sus conocimientos y por su paciencia.

Tabla de contenido

Lista de figuras

Lista de tablas

Anexos

Anexo 1: Artículo publicado. **Valero-Rubio, D.,** Jiménez, K. M., Fonseca, D. J., Payán-Gomez, C., & Laissue, P. (2018). **Transcriptomic analysis of FUCA1 knockdown in keratinocytes reveals new insights in the pathogenesis of fucosidosis skin lesions.** *Experimental Dermatology*. https://doi.org/10.1111/exd.13532

Anexo 2: Tabla de los genes desregulados en el microarreglo.

1. Resumen

La fucosidosis es una enfermedad huérfana de depósito lisosomal clasificada en dos subtipos según la gravedad de los signos y síntomas clínicos. Las anormalidades en la piel de los pacientes con fucosidosis incluyen angioqueratoma corporis difuso, telangiectasia esencial generalizada, hiperhidrosis e hipohidrosis, acrocianosis y bandas transversales en las uñas. Se ha descrito que >50% de los pacientes con fucosidosis presentan angioqueratomas. A nivel molecular, la fucosidosis es causada por mutaciones del gen alfa-L-fucosidasa 1 (*FUCA1*) el cual codifica para la enzima α-L-fucosidasa responsable de la hidrolisis de la fucosa. Obtener muestras para realizar estudios funcionales ha sido un reto por la dificultad de encontrar individuos afectados. El efecto de la disminución de *FUCA1* en la expresión de otros genes es desconocido.

El objetivo del presente trabajo de tesis fue analizar, en queratinocitos, el efecto transcriptómico global del silenciamiento del gen *FUCA1* en el marco de una mejor comprensión de la patogénesis de las lesiones cutáneas que afectan a los pacientes con fucosidosis. El silenciamiento de *FUCA1,* utilizando siRNA, se realizó en queratinocitos inmortalizados humanos (HaCaT). Para el análisis de la expresión genética a nivel transcriptómico global se usaron microarreglos de la plataforma de Affymetrix y ensayos de qPCR. Por medio de análisis bioinformáticos se realizó la agrupación funcional de los genes modificados luego del silenciamiento de *FUCA1*. 387 genes mostraron una expresión diferencial entre células silenciadas y las no silenciadas. 222 de estos genes se encontraron sobreexpresados y 165 regulados negativamente. Los genes diferencialmente expresados pertenecían a dos grupos principales: diferenciación de queratinocitos / desarrollo epidérmico (n=17) y respuesta inmune (n=61). Numerosos genes se encontraron diferencialmente

expresados entre las células transfectadas con siRNA-*FUCA1* y las células control. Este efecto podría haber sido producido, al menos en parte, por la expresión anormal de factores de transcripción como por ejemplo, *FOXN1*. Por lo tanto, proponemos que las lesiones cutáneas relacionadas con la fucosidosis (e.g. angioqueratoma) y las de otras enfermedades (e.g. psoriasis) pueden ser causadas por disfunciones en cascadas moleculares comunes superpuestas.

Por último, es importante señalar que numerosas publicaciones de nuestro grupo fundamentan y complementan los abordajes teóricos y experimentales citados en el trabajo presentado "Análisis transcriptómico global del silenciamiento de *FUCA1* en queratinocitos revela nuevos hallazgos sobre la patogénesis de las lesiones cutáneas de la fucosidosis" (Castro et al., 2013; Ducat et al., 2016; Fonseca et al., 2015; Forero et al., 2016; Laissue, 2015, 2018; Laissue et al., 2016; Laissue, Restrepo, & Ortiz, 2017; Mateus et al., 2017; Mitropoulos et al., 2015; O. Ortega-Recalde, Beltrán, et al., 2015; O. Ortega-Recalde, Moreno, et al., 2015; O. Ortega-Recalde, Silgado, Fetiva, Fonseca, & Laissue, 2016; Oscar Ortega-Recalde et al., 2013; Liliana C. Patiño et al., 2017, p. 1, 2017, p. 15; Liliana Catherine Patiño, Beau, et al., 2017; Liliana Catherine Patiño, Silgado, & Laissue, 2017; Prada & Laissue, 2014; Quintero-Ronderos et al., 2017; Valero-Rubio, Jiménez, Fonseca, Payán-Gomez, & Laissue, 2018; Vatin et al., 2014)

Según los lineamientos de la maestría con la publicación de un artículo científico en una revista indexada internacionalmente únicamente se contemplará en el escrito del trabajo de investigación los objetivos, la pregunta de investigación, los materiales y métodos, resultados, las conclusiones y las referencias.

2. Objetivos de la investigación

2.1.Objetivo general:

- Identificar nuevos mecanismos y actores moleculares potencialmente relacionados con la etiopatología de las lesiones cutáneas de pacientes con fucosidosis.

2.2. Objetivos específicos:

- Analizar en queratinocitos el efecto transcriptómico global del silenciamiento de *FUCA1*.
- Determinar qué procesos biológicos podrían estar afectados por el silenciamiento de *FUCA1* en un modelo celular pertinente para el estudio de lesiones cutáneas.

3. Pregunta científica

¿Cuál es el efecto a nivel transcriptómico global del silenciamiento de *FUCA1* en un modelo celular pertinente de tejido epidérmico?

4. Materiales y métodos

4.1. Cultivo celular, siembra y transfección.

4.1.1. Línea celular HaCaT

La línea celular HaCaT (Human adult low Calcium high Temperature) provienen de células de queratinocitos de piel humana adulta, que se cultivan habitualmente a concentraciones bajas de calcio y altas temperaturas. Esta línea fue inmortalizada mediante la infección con el virus de simio-40 (SV40) o la transfección con su DNA (Boukamp et al., 1988). El virus SV40 expresa el antígeno T el cual produce la inactivación de genes supresores de tumores y la estabilización telomérica, procesos relacionados con el desarrollo del cáncer (Jha, Banga, Palejwala, & Ozer, 1998; Steinberg & Defendi, 1983).

Esta línea celular expresa propiedades de las células no inmortalizadas, posee facilidad de diferenciación y permiten el estudio de diferentes patologías a nivel de la piel (Wilson, 2014).

4.1.2. Cultivo celular

Las células HaCaT se cultivaron en cajas de cultivo celular T75 con medio DMEM (Dubbelco´s Modified Eagle Medium) suplementado con 10% de suero fetal bovino (SFB), penicilina 5000U/ml, 5mg/ml de estreptomicina, en una atmósfera de 5% de CO_2 y una temperatura de 37°C. Una vez las células se encontraron en una confluencia entre el 80% y el 90% se retiró el medio de cultivo, se realizó un lavado con PBS 1X (buffer fosfato salino) y se desprendieron las células incubando con tripsina durante 10 minutos a 37°C. Posteriormente, las células se recolectaron agregando 5ml de medio DMEM y centrifugando a 1500rpm durante 4 minutos.

El pellet de células obtenido se diluyó en un volumen apropiado de medio DMEM para realizar conteo celular utilizando una cámara de Neubauer. En una placa de 6 pozos se sembraron 4 de ellos (200.000 células/pozo) con 2ml de medio de crecimiento suplementado con suero fetal bovino y libre de antibiótico. Se obtuvo una confluencia de 70% 24 horas luego de la siembra.

4.1.3. Transfección de siRNA dirigidos al gen *FUCA1*

La transfección es el proceso por el cual se inserta un ácido nucleico de interés en células diana (Homann et al., 2017). Existen diferentes métodos para introducir el material genético: físicos, químicos y biológicos (Homann et al., 2017).

Para la transfección se utilizaron dos tipos de siRNA: siRNA duplex dirigido al gen *FUCA1* (sc 78583) y siRNA-A (scramble) como control de silenciamiento (sc 37007) los cuales fueron obtenidos de la casa comercial Santacruz Biotecnology. Estos son incorporados a la célula mediante la acción del reactivo de transfección (sc 29528) basado en lípidos.

Para cada ensayo de transfección se realizaron dos soluciones (solución A y B) (tabla1):

Tabla 1: Soluciones usadas para la transfección con siRNA.

Solución A		**Solución B**	
Cantidad	**Reactivo**	**Cantidad**	**Reactivo**
80pmol/pozo	siRNA-*FUCA1* o siRNA-A	8ul/pozo	Reactivo de transfección
100µl	Medio de transfección	100µl	Medio de transfección

Posteriormente, se mezcló la solución A directamente con la solución B y se incubó durante 45 minutos a temperatura ambiente.

Se visualizaron las células sembradas y se realizó un lavado con 2ml de medio de transfección. Se retiró el medio y se agregó 800µl/pozo de medio de transfección y 200µl/pozo de la mezcla de siRNA (solución A y B). Se incubó durante 5 horas a 37°C.

Pasado el tiempo de incubación se añadió 1ml de medio DMEM suplementado con 20% de suero fetal bovino (SFB) y 2X de antibiótico sin retirar la mezcla de transfección. Se dejó en incubación durante 24 horas a 37°C. Cumplido este tiempo, se retiró el medio y se reemplazó con DMEM suplementado con 10% de SFB y 1X de antibiótico. Las células se incubaron durante 60 horas a 37°C.

Luego del tiempo de incubación se retiró el medio, se realizó un lavado con PBS 1X, se agregaron 250µl de trizol/pozo y se recogió la suspensión celular en tubos Eppendorf para realizar la extracción de RNA total.

4.2. Extracción de RNA

Las diferentes suspensiones celulares en Trizol, obtenidas de los experimentos de transfección, fueron utilizadas para realizar la extracción de RNA total, utilizando el kit comercial Purelink RNA Mini Kit (ThermoFisher Scientific). Se siguió el protocolo descrito por el fabricante.

Brevemente, se agregaron 200µl de cloroformo/ml de trizol y se mezcló por inmersión durante 15 segundos. La mezcla se incubó a temperatura ambiente 3 minutos y se centrifugó a 12000*xg* durante 15 minutos a 4°C. La fase superior (acuosa) se transfirió a un tubo Eppendorf nuevo (aproximadamente 400µl), se agregó un volumen igual de etanol 70% y se

mezcló por inmersión durante 30 segundos. Se transfirieron 700µl de la mezcla a un tubo de recolección con columna y se centrifugó a 12000*xg* durante 15 segundos a temperatura ambiente. Posteriormente, se realizaron los lavados de la columna con el *buffer Wash* I y II del kit. Finalmente, el RNA se eluyó de la columna con 30µl de agua libre de RNasa.

La cantidad y calidad del RNA fue verificada con el Bioanalyzer 2100 (version 2.6) (Agilent, Santa Clara, CA, EE.UU).

4.3. Síntesis de cDNA y RT-PCR

El cDNA de doble cadena se sintetizó a partir del RNA total extraído previamente utilizando el kit de transcriptasa inversa SuperScript III First-Strand Synthesis System (Invitrogen) según protocolo del fabricante.

Para 500ng/µl de RNA total se mezcló 1µl de oligo dT, con 1 µl de dNTP y H20 para obtener un volumen final de 10µl. Se incubó durante 5 minutos a 65°C y en hielo durante 1 minuto. Para la mezcla de síntesis de cDNA se utilizó 2µl de buffer 10X, 4µl de $MgCl_2$, 2µl de DTT, 1µl de RNAsaOUT (40U/µl) y 1µl de Superscript III (200U/µl). Posteriormente se integró la mezcla de incubación con 10µl de la mezcla de síntesis de cDNA y se incubaron durante 50 minutos a 50°C. Para terminar la reacción de síntesis se dejó incubando 85°C durante 5 minutos. Finalmente se añadió 1µl de RNasa H y se incubó a 37° durante 20 minutos.

Para evaluar cualitativamente el nivel de silenciamiento utilizando siRNA, se realizó amplificación de *FUCA1*, por PCR del cDNA obtenido de la transfección. Se utilizaron dos pares de primers comerciales de Santa Cruz Biotechnology: A *Fuca1* (h), que amplifica un fragmento de aproximadamente 600pb y B *Fuca1* (h) que amplifica un fragmento de aproximadamente 200pb. Adicionalmente se utilizaron primers para la amplificación del gen

GAPDH usado como control. La reacción de PCR se realizó en un volumen final de 25µl, con 12,5 µl de Master Mix (Promega), 2µl de cDNA (100ng) y 10 µM de cada par de primers, siguiendo el programa (tabla 2).

Tabla 2: programa para la amplificación por PCR del gen *Fuca1*

Paso	Temperatura	Tiempo	Ciclos
Desnaturalización inicial	94°C	10 Minutos	
Desnaturalización	94°C	40 Segundos	30c
Anillamiento	58°C	40 Segundos	
Extensión	72°C	40 Segundos	
Extensión final	72°C	10 Minutos	

4.4. Microarreglos de expresión

El efecto transcriptómico secundario al silenciamiento del gen *FUCA1* se analizó con el RNA extraído de las dos condiciones (células silenciadas (TSC), células control (NTC)) usando el microarray de Affymetrix GeneChip Primeview human gene expression arrays (Thermo Fisher, Waltham, MA. Ref. 901837). Estos experimentos, se realizaron en el Instituto para la investigación en biomedicina (*IRB*, Barcelona, España).

Se procesó un total de doce muestras entre réplicas técnicas y biológicas (Figura 1):

Figura 1: Muestras procesadas para el análisis del microarreglo. RB: replica biológica. RT: Replica técnica. TSC: células transfectadas con siRNA- *FUCA1*. NTC: células transfectadas

con secuencia scramble siRNA-A (control negativo).

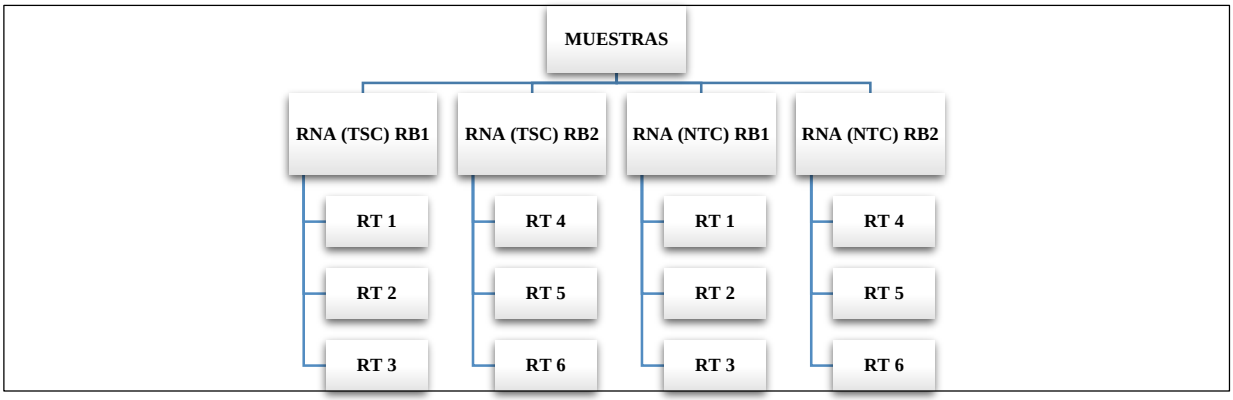

Para el procesamiento y el análisis del microarray, como primer paso se realizó la síntesis y la amplificación de cDNA. Posteriormente, se llevó a cabo la fragmentación y marcaje del material genético. Luego, se efectuó el proceso de hibridación del total de las muestras durante toda la noche. Se formaron grupos de cuatro muestras para el paso de lavado y escáner teniendo en cuenta una correcta distribución de las muestras. Finalmente, se obtuvo la imagen del ensayo y se realizó el análisis y la interpretación de los resultados.

4.5. Control de calidad y análisis de ontología génica.

Para realizar los estudios de expresión génica y por la labilidad e inestabilidad del RNA lo primero que se verificó fue su calidad. Esta, se determinó mediante la medición del número de integridad del RNA (RIN) de acuerdo a una escala que se extiende desde 1 para RNA degradados hasta 10 para ARN intactos. Este ejercicio se realizó por medio del Bioanalyzer 2100 (versión 2.6) (Agilent, Santa Clara, CA, EE.UU) (Schroeder et al., 2006)

Posteriormente, luego de obtener los resultados del microarreglo y basados en los archivos .CEL de cada condición se realizó el análisis del control de calidad. Éste se desarrolló usando la herramienta bioinformática Arrayanalisis.org (http://arrayanalysis.org). De esta forma se

puede determinar la hibridación de cada una de las sondas en las diferentes matrices, la calidad de la señal de intensidad y generar una correlación entre los diferentes grupos o condiciones del estudio (Eijssen et al., 2013).

Adicionalmente, para proponer una interpretación biológica de los resultados obtenidos del microarray se realizó una agrupación funcional (clustering) usando los genes diferencialmente expresados y tomando de manera independiente aquellos que se encontraban sobre y sub expresados (Hong, Zhang, Li, Shen, & Guo, 2014). Este análisis se realizó utilizando el software DAVID (https://david.ncifcrf.gov). Esta herramienta bioinformática permite agrupar los genes de acuerdo a su relación funcional. Los grupos funcionales se generan por los procesos biológicos con los que están asociados la totalidad de los genes en la lista.

4.6. Ensayos de PCR cuantitativa (qPCR)

Para la validación de los resultados obtenidos del experimento de microarray, se realizó qPCR. Se escogieron 16 genes expresados diferencialmente: *FUCA1, KRT4, KRT1, KRT16, TGM1, EDAR, S100A7, OVOL1, SCEL, SPRR2A, SPRR2D, IRF9, IRF1, GBP2, ICAM1, IFI27.* La secuencia de los primers de cada uno de los genes se obtuvo de la base de datos Primer Bank (Tabla 3) por ser un repositorio con un número importante de primers para qPCR comprobados y verificados experimentalmente.

Tabla 3: Secuencia de primers usados en qPCR. Obtenidos de: Primer Bank (http://pga.mgh.harvard.edu/primerbank/).

Gene	Primer sequence (5´- 3´)	Amplicon Size (bp)	Tm (°C)
FUCA 1	F: GAAGCCAAGTTCGGGGTGTT	131	62

	R: GGGTAGTTGTCGCGCATGA		62
KRT4	F: CGCGAACAGATCAAGCTCCT	148	62
	R: GGGGCTCAAGGTTTTTGCTG		61
TGM1	F: GCACCACACAGACGAGTATGA	109	61
	R: GGTGATGCGATCAGAGGATTC		60
EDAR	F: CAGCCCGAGCGGAATACTC	121	62
	R: CCGTAGCCACAGGACAGGTA		62
SCEL	F: TCGGTACAGTTCTGATGACACT	114	60
	R: AACATGGACATGCTCCTATTGG		60
OVOL1	F: TGAACATGAGCCTTCGAGACT	147	60
	R: CAAGGGTCACCTTCATCTTGG		60
IFI27	F: TGCTCTCACCTCATCAGCAGT	115	62
	R: CACAACTCCTCCAATCACAACT		60
IRF9	F: GCCCTACAAGGTGTATCAGTTG	84	60
	R: TGCTGTCGCTTTGATGGTACT		61
IRF1	F: ATGCCCATCACTCGGATGC	204	62
	R: CCCTGCTTTGTATCGGCCTG		62
GBP2	F: CTATCTGCAATTACGCAGCCT	182	60
	R: TGTTCTGGCTTCTTGGGATGA		61
ICAM1	F: ATGCCCAGACATCTGTGTCC	112	61
	R: GGGGTCTCTATGCCCAACAA		61
KRT1	F: CCCAGTACGAGGATATAGCCC	149	60
	R: GATCACACGATTCAGCTCAGAA		60
KRT16	F: GACCGGCGGAGATGTGAAC	91	62
	R: CTGCTCGTACTGGTCACGC		62
S100A7	F: TCCAAACACACACATCTCACTCA	113	60
	R: CGATCATGCCTATTATGGACCTCT		60
SPRR2A	F: GATATTTGGCTCACCTCGTTCCA	103	61
	R: TGGGCAGATTACTGGCTAAGGAG		61
SPRR2D	F: CTTTCTCCTTAACCTGTGGCCTG	109	61
	R: GGACTTCCTTTTCTTAGCTCCACC		61

La reacción de PCR se realizó en un volumen final de 20µl, con 20 ng/µl de cDNA, 1X SYBR Green PCR Master Mix (Applied Biosystems) 0.4 µM de primers y 6.5 ul de agua. El ensayo se realizó usando una curva estándar y análisis de curva de melting para verificar la especificidad de los primers y siguiendo el programa de la Tabla 4.

Tabla 4: programa para qPCR de los 16 genes escogidos para la validación del comportamiento transcriptómico.

Paso	Temperatura	Tiempo	Ciclos
Activación de la polimerasa	94°C	10 Minutos	
Desnaturalización	95°C	30 Segundos	40c
Anillamiento	61°C	30 Segundos	
Extensión-Obtención de Señal	72°C	25Segundos	

4.7. Estudios estadísticos y bioinformáticos

El análisis de expresión diferencial de las condiciones del estudio (TSC-NTC) se realizó con el software R 3.0.0 (www.r-project.org) a partir de los archivos .CEL generados por la plataforma de Affymetrix. Teniendo en cuenta que los datos obtenidos del microarreglo se encontraban representados en log2 se realizó una resta para obtener la relación entre las condiciones. Resultados de +1 corresponden a 2 veces más o dos veces menos expresados (-1).

El análisis estadístico de los datos se realizó mediante SPSS (version 24, SPSS Inc.). Para establecer potenciales diferencias estadísticamente significativas los ensayos de qPCR se usó la prueba estadística t-student y se determinó la diferencia en el nivel de expresión entre cada condición (TSC-NTC).

5. Resultados

5.1. RT-PCR y qPCR de *FUCA1* en células transfectadas con siRNA.

Se analizó por medio de RT-PCR el silenciamiento del gen *FUCA1* luego de la transfección del siRNA. Se observó una notable diferencia en la intensidad de las bandas de cada una de las condiciones (TSC, NTC), siendo menor la correspondiente a las células transfectadas con 80pmol de siRNA. (Figura 2 (a)).

Por medio de qPCR se obtuvo el resultado de cuantificación de $2.36x10^{10}$ correspondiente al número de copias del gen presente en las células silenciadas. Se observó una diferencia estadísticamente significativa ($p<0.001$) respecto al número de copias en las células control ($2.37x10^{11}$). (Figura 2 (b)).

Figura 2. Silenciamiento de *FUCA1*. **(a)** Resultados de RT-PCR de *FUCA1* **(b)** Cuantificación del número de copias de *FUCA1* mediante qPCR *** valor de p <0.001. TSC: células transfectadas con siRNA- *FUCA1*. NTC: células transfectadas con el control negativo (secuencia scramble siRNA-A). L: Marcador de peso molecular

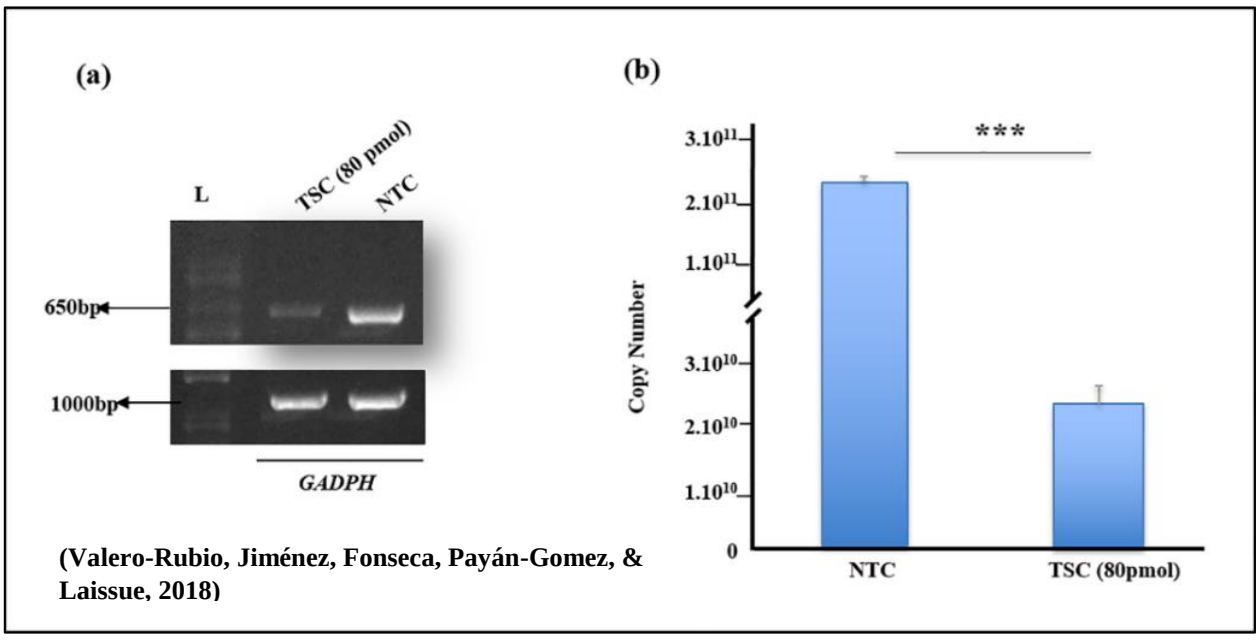

(Valero-Rubio, Jiménez, Fonseca, Payán-Gomez, & Laissue, 2018)

5.2.Control de calidad del material genético y de los resultados del microarreglo

Se encontró una buena calidad de ARN con algunas diferencias en cuanto a la probable cantidad para cada una de las muestras. Se obtuvieron resultados satisfactorios para el número de integridad de cada RNA (RIN) (entre 9.1 y10) (Figura 3).

Figura 3: Resultados de la medición de la integridad del RNA (RIN) de las muestras. TSC: células transfectadas con siRNA- *FUCA1*. NTC: células transfectadas con secuencia scramble siRNA-A (control negativo).

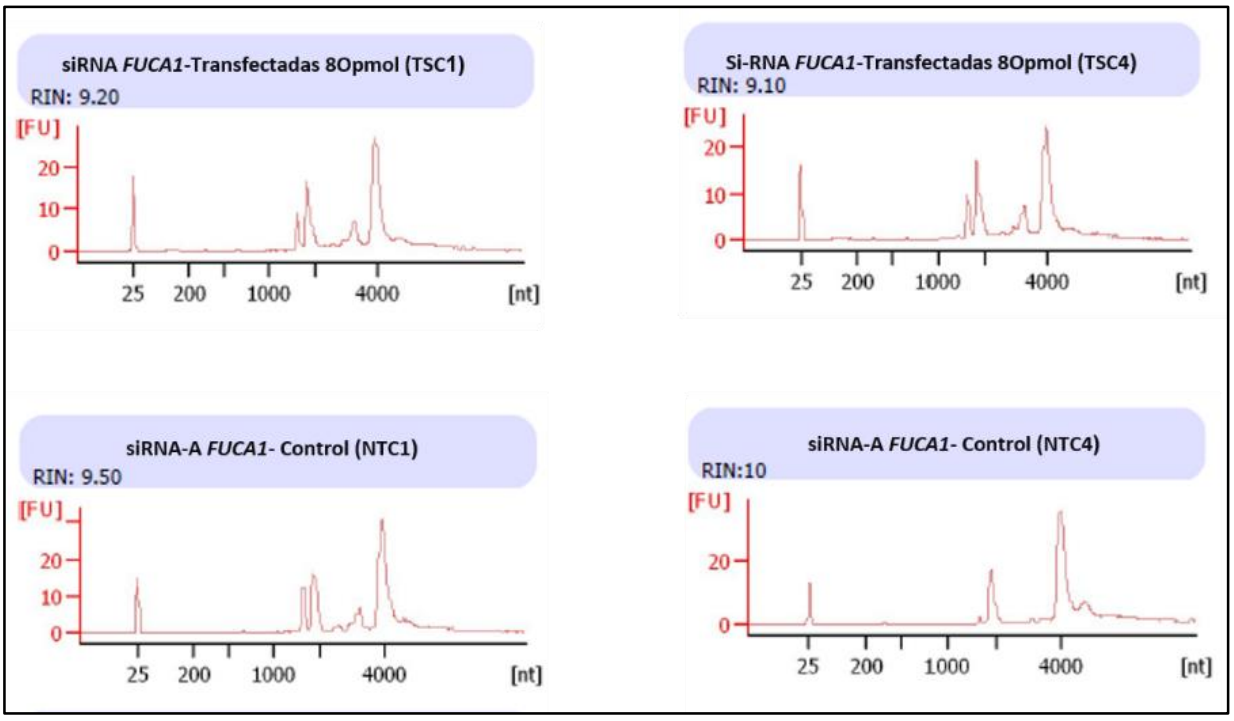

Posteriormente, se realizó el control de calidad de los resultados obtenidos del microarreglo. Se obtuvieron resultados que mostraron una excelente calidad en cuanto a la señal y la hibridación de las sondas de acuerdo a la intensidad generada por los controles positivos y negativos para cada matriz (Figura 4 (a)). Se encontró además que existía una buena homogeneidad en la distribución de cada una de las sondas en los diferentes arrays (Figura 4

(b)). En el análisis de correlación de las diferentes expresiones entre las matrices se ilustraron los cambios generados en las células por cada condición en el experimento mostrando dos poblaciones celulares con características diferentes que distinguían las células TSC de las células NTC (Figura 4 (c)).

Figura 3: Control de calidad de los resultados del microarreglo.

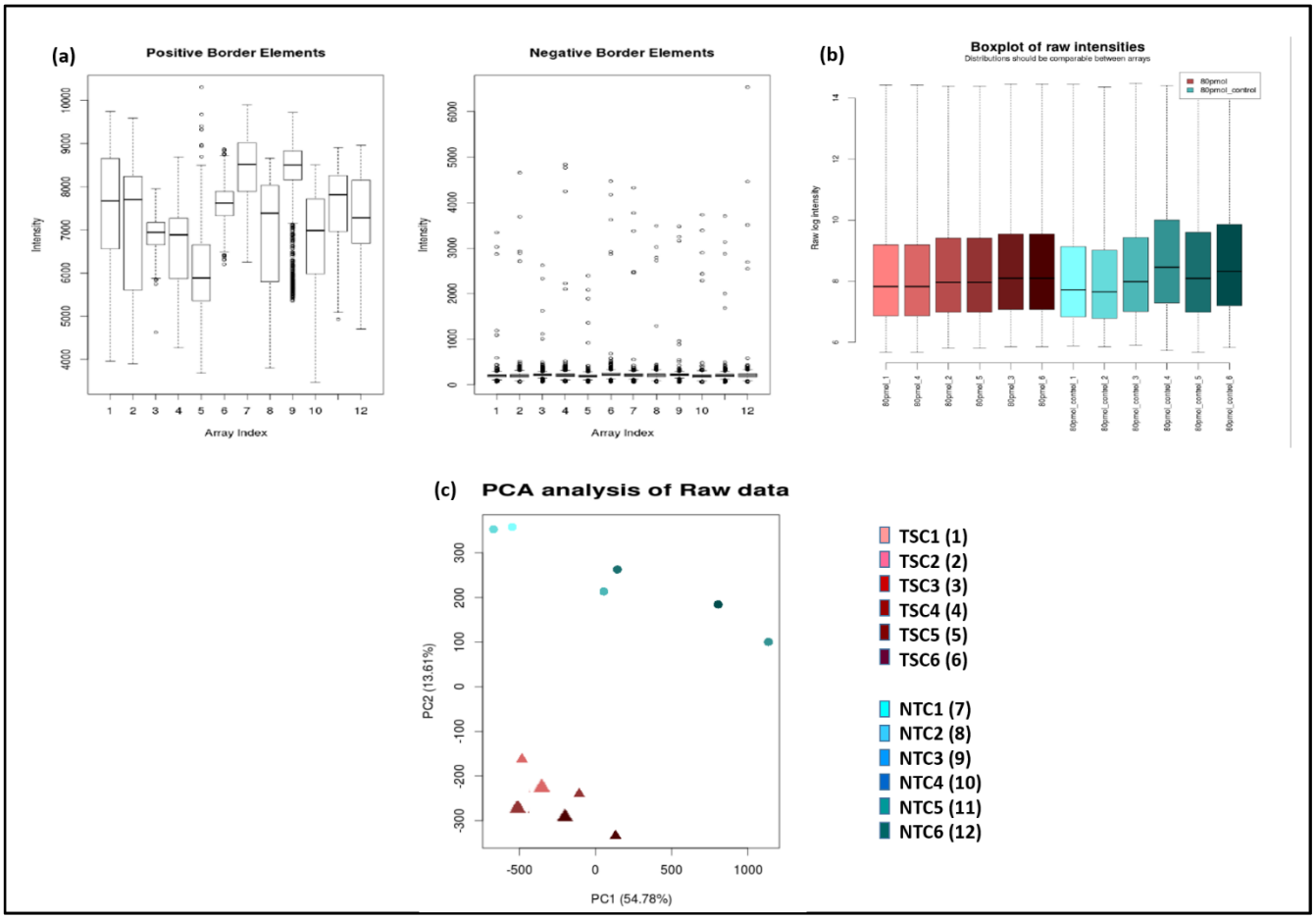

5.3. Análisis de los genes diferencialmente expresados entre las células transfectadas con siRNA (TSC) y las células control (NTC), usando microarreglos de expresión y clusterización funcional

En el análisis comparativo de la expresión génica (mediante R) entre TSC-NTC se encontraron 387 genes diferencialmente expresados (Anexo 2). De estos, 222 correspondían a genes sobre expresados y 165 a genes reprimidos.

Se obtuvieron mediante DAVID, para los genes sobre expresados, 12 categorías relacionadas con diferentes procesos biológicos. De estas categorías, por su similaridad, se realizó una reasignación de algunas de ellas para generar dos grupos principales: diferenciación de queratinocitos/ desarrollo epidérmico (conformado por 17 genes) y respuesta inmune (61 genes) (Figura 5).

Figura 5: Agrupamiento funcional de los genes sobreexpresados.

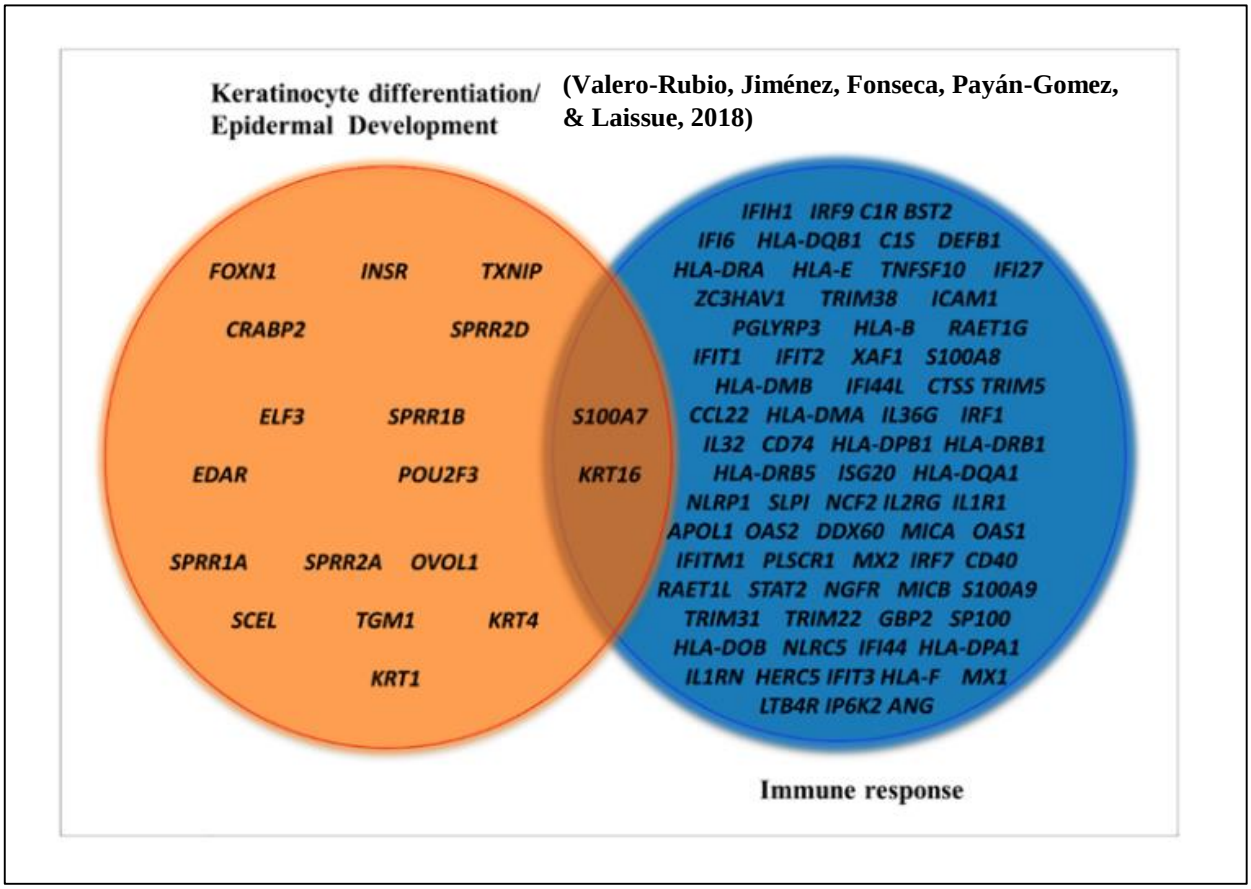

Se realizó un mapa de calor que mostró la diferencia en el nivel de expresión de cada uno de los genes de las categorías funcionales de las células silenciadas respecto a las células control (Figura 6).

Figura 6: Mapa de calor. (a) expresión de los genes presentes en la respuesta inmune en las células silenciadas con respecto a su expresión en las células control. (b) Genes presentes en el grupo funcional de diferenciación de queratinocitos/ desarrollo epidérmico. TSC: células transfectadas con *FUCA1*- siRNA. NTC: células transfectadas con secuencia scramble siRNA-A (control negativo).

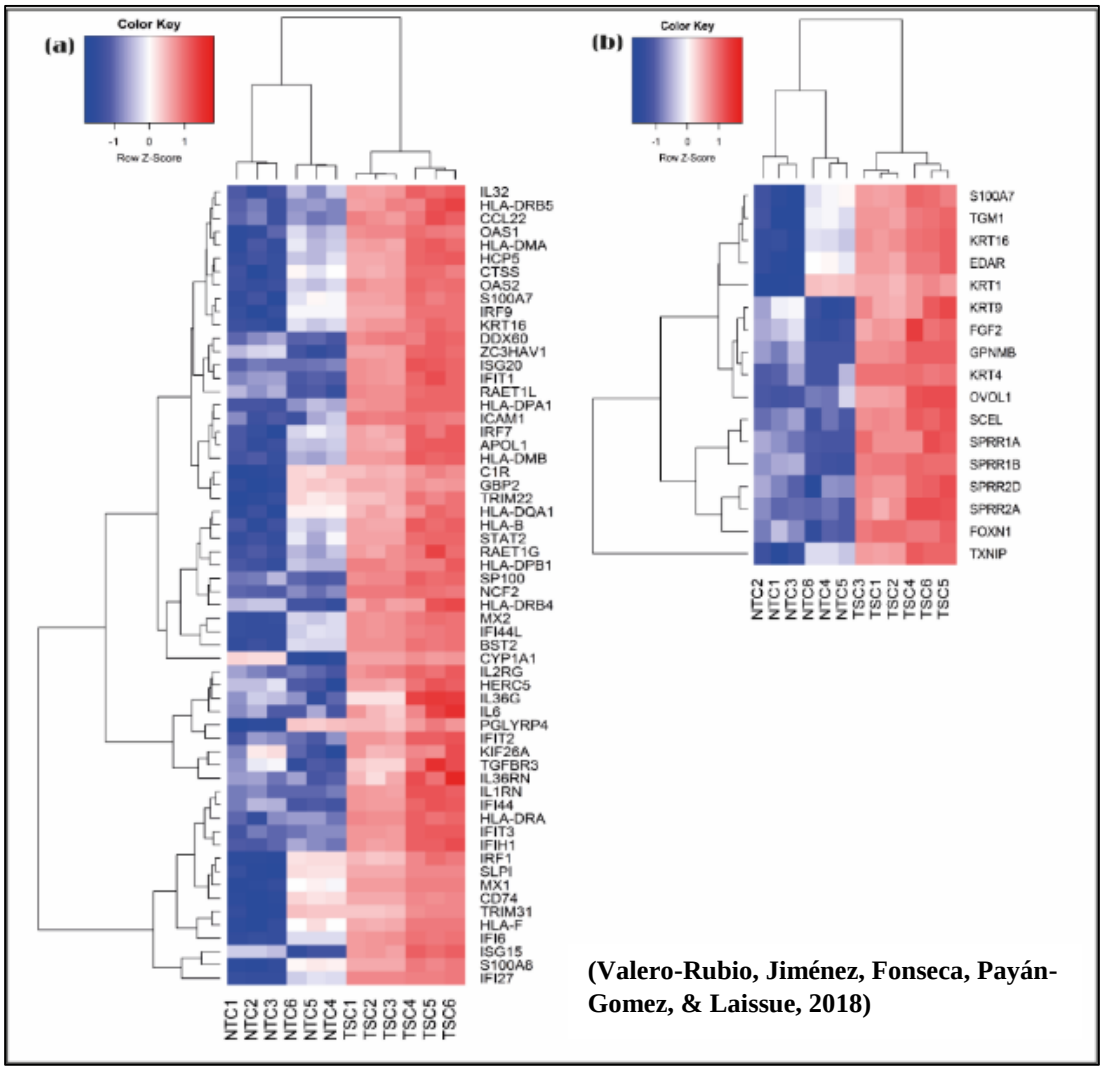

FOXN1, *ELF3*, *POU2F3*, *STAT2* son factores de transcripción que se encontraron sobre-expresados en las células transfectadas con siRNA- *FUCA1*. La expresión anormal en estos factores podría alterar la regulación de diferentes genes diana y cascadas moleculares.

Con respecto a los 165 genes inhibidos no se pudo establecer ningún proceso biológico o categoría funcional de importancia.

5.4.Verificación de los resultados del microarreglo mediante qPCR.

En los experimentos de qPCR se mostró un comportamiento similar de los genes sobre y subexpresados al obtenido en el microarreglo (Figura 7).

Figura 7: qPCR de 16 genes ** valor de p <0.01 *** valor de p <0.001. TSC: células transfectadas con *FUCA1* siRNA. NTC: células transfectadas con secuencia scramble siRNA-A (control negativo).

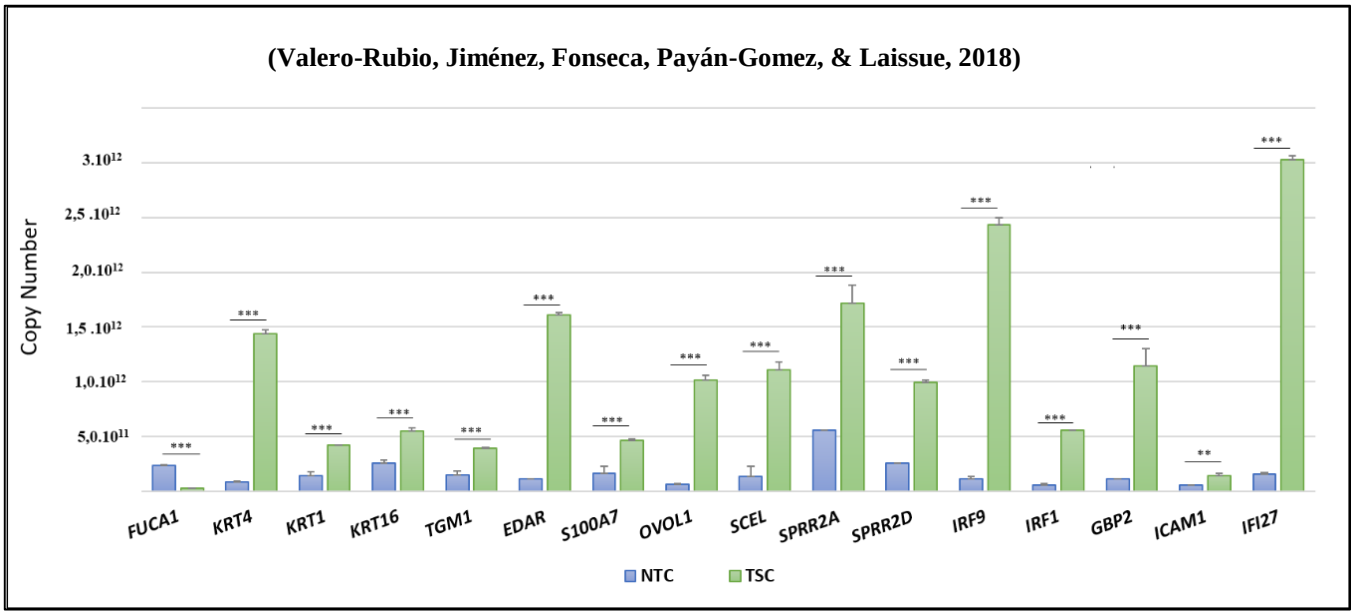

6. Conclusiones

- La sobreexpresión de genes relacionados con la diferenciación de queratinocitos y el desarrollo epidérmico tras el silenciamiento del gen *FUCA1* puede en parte explicar la presencia fenotípica de angiokeratomas en pacientes con fucosidosis.
- La sobreexpresión de factores de transcripción como *FOXN1* podría estar asociada a la desregulación de diferentes genes como *FLG, MMP7o CCL27.*
- Se cree que *FOXN1* puede generar una función importante en la fisiopatología de las lesiones de piel en pacientes con fucosidosis.
- **Los resultados de esta tesis fueron publicados el 8 de marzo del 2018 en la revista Experimental Dermatology clasificada como Q1 según SCImago Journal Rank (SJR) doi: 10.1111/exd.13532**

Referencias:

Boukamp, P., Petrussevska, R. T., Breitkreutz, D., Hornung, J., Markham, A., & Fusenig, N. E. (1988). Normal keratinization in a spontaneously immortalized aneuploid human keratinocyte cell line. *The Journal of Cell Biology*, *106*(3), 761-771.

Castro, T., Mateus, H. E., Fonseca, D. J., Forero, D., Restrepo, C. M., Talero, C., … Laissue, P. (2013). Sequence analysis of the ADRA2A coding region in children affected by attention deficit hyperactivity disorder. *Neurological Sciences: Official Journal of the Italian Neurological Society and of the Italian Society of Clinical Neurophysiology*, *34*(12), 2219-2222. https://doi.org/10.1007/s10072-013-1569-4

Ducat, A., Doridot, L., Calicchio, R., Méhats, C., Vilotte, J.-L., Castille, J., … Vaiman, D. (2016). Endothelial cell dysfunction and cardiac hypertrophy in the STOX1 model of preeclampsia. *Scientific Reports*, *6*, 19196. https://doi.org/10.1038/srep19196

Eijssen, L. M. T., Jaillard, M., Adriaens, M. E., Gaj, S., Groot, D., J, P., … Evelo, C. T. (2013). User-friendly solutions for microarray quality control and pre-processing on ArrayAnalysis.org. *Nucleic Acids Research*, *41*(W1), W71-W76. https://doi.org/10.1093/nar/gkt293

Exome Sequencing Is an Efficient Tool for Variant Late-Infantile Neuronal Ceroid Lipofuscinosis Molecular Diagnosis. (s. f.). Recuperado 30 de abril de 2018, a partir de http://journals.plos.org/plosone/article?id=10.1371/journal.pone.0109576

Fonseca, D. J., Patiño, L. C., Suárez, Y. C., de Jesús Rodríguez, A., Mateus, H. E., Jiménez, K. M., … Laissue, P. (2015). Next generation sequencing in women affected by nonsyndromic premature ovarian failure displays new potential

causative genes and mutations. *Fertility and Sterility*, *104*(1), 154-162.e2. https://doi.org/10.1016/j.fertnstert.2015.04.016

Forero, D. A., Wonkam, A., Wang, W., Laissue, P., López-Correa, C., Fernández-López, J. C., … Perry, G. (2016). Current needs for human and medical genomics research infrastructure in low and middle income countries. *Journal of Medical Genetics*, *53*(7), 438-440. https://doi.org/10.1136/jmedgenet-2015-103631

Homann, S., Hofmann, C., Gorin, A. M., Nguyen, H. C. X., Huynh, D., Hamid, P., … Kelesidis, T. (2017). A novel rapid and reproducible flow cytometric method for optimization of transfection efficiency in cells. *PLoS ONE*, *12*(9). https://doi.org/10.1371/journal.pone.0182941

Hong, G., Zhang, W., Li, H., Shen, X., & Guo, Z. (2014). Separate enrichment analysis of pathways for up- and downregulated genes. *Journal of The Royal Society Interface*, *11*(92), 20130950. https://doi.org/10.1098/rsif.2013.0950

Jha, K. K., Banga, S., Palejwala, V., & Ozer, H. L. (1998). SV40-Mediated immortalization. *Experimental Cell Research*, *245*(1), 1-7. https://doi.org/10.1006/excr.1998.4272

Laissue, P. (2015). Aetiological coding sequence variants in non-syndromic premature ovarian failure: From genetic linkage analysis to next generation sequencing. *Molecular and Cellular Endocrinology*, *411*, 243-257. https://doi.org/10.1016/j.mce.2015.05.005

Laissue, P. (2018). The molecular complexity of primary ovarian insufficiency aetiology and the use of massively parallel sequencing. *Molecular and Cellular Endocrinology*, *460*, 170-180. https://doi.org/10.1016/j.mce.2017.07.021

Laissue, P., Lakhal, B., Vatin, M., Batista, F., Burgio, G., Mercier, E., … Vaiman, D. (2016). Association of FOXD1 variants with adverse pregnancy outcomes in mice and humans. *Open Biology*, *6*(10). https://doi.org/10.1098/rsob.160109

Laissue, P., Restrepo, C. M., & Ortiz, A. M. (2017). Improving the evaluation of milestones for students completing a clinical genetics elective. *Genetics in Medicine*, *19*(12). https://doi.org/10.1038/gim.2017.62

Mateus, H. E., Pérez, A. M., Mesa, M. L., Escobar, G., Gálvez, J. M., Montaño, J. I., … Laissue, P. (2017). A first description of the Colombian national registry for rare diseases. *BMC Research Notes*, *10*(1), 514. https://doi.org/10.1186/s13104-017-2840-1

Mitropoulos, K., Al Jaibeji, H., Forero, D. A., Laissue, P., Wonkam, A., Lopez-Correa, C., … Patrinos, G. P. (2015). Success stories in genomic medicine from resource-limited countries. *Human Genomics*, *9*, 11. https://doi.org/10.1186/s40246-015-0033-3

Ortega-Recalde, O., Beltrán, O. I., Gálvez, J. M., Palma-Montero, A., Restrepo, C. M., Mateus, H. E., & Laissue, P. (2015). Biallelic HERC1 mutations in a syndromic form of overgrowth and intellectual disability. *Clinical Genetics*, *88*(4), e1-3. https://doi.org/10.1111/cge.12634

Ortega-Recalde, O., Fonseca, D. J., Patiño, L. C., Atuesta, J. J., Rivera-Nieto, C., Restrepo, C. M., … Laissue, P. (2013). A novel familial case of diffuse leukodystrophy related to NDUFV1 compound heterozygous mutations. *Mitochondrion*, *13*(6), 749-754. https://doi.org/10.1016/j.mito.2013.03.010

Ortega-Recalde, O., Moreno, M. B., Vergara, J. I., Fonseca, D. J., Rojas, R. F., Mosquera, H., … Laissue, P. (2015). A novel TGM1 mutation, leading to multiple splicing

rearrangements, is associated with autosomal recessive congenital ichthyosis. *Clinical and Experimental Dermatology*, *40*(7), 757-760. https://doi.org/10.1111/ced.12627

Ortega-Recalde, O., Silgado, D., Fetiva, C., Fonseca, D. J., & Laissue, P. (2016). Transcriptomic analysis of skin in a case of ichthyosis Curth-Macklin caused by a KRT1 mutation. *The British Journal of Dermatology*, *175*(6), 1372-1375. https://doi.org/10.1111/bjd.14969

Patiño, L. C., Beau, I., Carlosama, C., Buitrago, J. C., González, R., Suárez, C. F., … Laissue, P. (2017). New mutations in non-syndromic primary ovarian insufficiency patients identified via whole-exome sequencing. *Human Reproduction (Oxford, England)*, *32*(7), 1512-1520. https://doi.org/10.1093/humrep/dex089

Patiño, L. C., Silgado, D., & Laissue, P. (2017). A potential functional association between mutant BMPR2 and primary ovarian insufficiency. *Systems Biology in Reproductive Medicine*, *63*(3), 145-149. https://doi.org/10.1080/19396368.2017.1291767

Patiño, L. C., Walton, K. L., Mueller, T. D., Johnson, K. E., Stocker, W., Richani, D., … Harrison, C. A. (2017). BMP15 Mutations Associated With Primary Ovarian Insufficiency Reduce Expression, Activity, or Synergy With GDF9. *The Journal of Clinical Endocrinology and Metabolism*, *102*(3), 1009-1019. https://doi.org/10.1210/jc.2016-3503

Prada, C. F., & Laissue, P. (2014). A high resolution map of mammalian X chromosome fragile regions assessed by large-scale comparative genomics. *Mammalian Genome: Official Journal of the International Mammalian Genome Society*, *25*(11-12), 618-635. https://doi.org/10.1007/s00335-014-9537-8

Quintero-Ronderos, P., Mercier, E., Fukuda, M., González, R., Suárez, C. F., Patarroyo, M. A., … Laissue, P. (2017). Novel genes and mutations in patients affected by recurrent pregnancy loss. *PloS One*, *12*(10), e0186149. https://doi.org/10.1371/journal.pone.0186149

Schroeder, A., Mueller, O., Stocker, S., Salowsky, R., Leiber, M., Gassmann, M., … Ragg, T. (2006). The RIN: an RNA integrity number for assigning integrity values to RNA measurements. *BMC Molecular Biology*, *7*, 3. https://doi.org/10.1186/1471-2199-7-3

Steinberg, M. L., & Defendi, V. (1983). Transformation and immortalization of human keratinocytes by SV40. *The Journal of Investigative Dermatology*, *81*(1 Suppl), 131s-6s.

Valero-Rubio, D., Jiménez, K. M., Fonseca, D. J., Payán-Gomez, C., & Laissue, P. (2018). Transcriptomic analysis of FUCA1 knockdown in keratinocytes reveals new insights in the pathogenesis of fucosidosis skin lesions. *Experimental Dermatology*. https://doi.org/10.1111/exd.13532

Vatin, M., Bouvier, S., Bellazi, L., Montagutelli, X., Laissue, P., Ziyyat, A., … Gris, J.-C. (2014). Polymorphisms of human placental alkaline phosphatase are associated with in vitro fertilization success and recurrent pregnancy loss. *The American Journal of Pathology*, *184*(2), 362-368. https://doi.org/10.1016/j.ajpath.2013.10.024

Whole-Exome Sequencing Enables Rapid Determination of Xeroderma Pigmentosum Molecular Etiology. (s. f.). Recuperado 30 de abril de 2018, a partir de http://journals.plos.org/plosone/article?id=10.1371/journal.pone.0064692

Wilson, V. G. (2014). Growth and differentiation of HaCaT keratinocytes. *Methods in Molecular Biology (Clifton, N.J.)*, *1195*, 33-41. https://doi.org/10.1007/7651_2013_42

ANEXOS

Anexo 1:

Artículo publicado. **Valero-Rubio, D**., Jiménez, K. M., Fonseca, D. J., Payán-Gomez, C., & Laissue, P. (2018). **Transcriptomic analysis of FUCA1 knockdown in keratinocytes reveals new insights in the pathogenesis of fucosidosis skin lesions**. *Experimental Dermatology*. https://doi.org/10.1111/exd.13532

PROF. PAUL LAISSUE (Orcid ID : 0000-0003-4180-4796)

Article type : Regular Article

Transcriptomic analysis of *FUCA1* knockdown in keratinocytes reveals new insights in the pathogenesis of fucosidosis skin lesions

Danyela Valero-Rubio [1], Karen Marcela Jiménez [1], Dora Janeth Fonseca [1], César Payán-Gomez [2] and Paul Laissue [1]

[1] Center For Research in Genetics and Genomics-CIGGUR. GENIUROS Research Group.

School of Medicine and Health Sciences, Universidad del Rosario. Bogotá. Colombia.

[2] Facultad de Ciencias Naturales y Matemáticas, Universidad del Rosario, Bogotá. Colombia.

***Corresponding author: Paul Laissue**

Center For Research in Genetics and Genomics-CIGGUR. GENIUROS Research Group.

School of Medicine and Health Sciences, Universidad del Rosario. Colombia.

Address: Carrera 24 N° 63C-69, Bogotá, Colombia.

Tel : +57 1 3474570

Fax : +57 1 3474570

E-mail: paul.laissue@urosario.edu.co

This article has been accepted for publication and undergone full peer review but has not been through the copyediting, typesetting, pagination and proofreading process, which may lead to differences between this version and the Version of Record. Please cite this article as doi: 10.1111/exd.13532

Abstract

Fucosidosis is a rare lysosomal storage disease which has been classified into two subtypes, depending on the severity of clinical signs and symptoms. Fucosidosis patients' skin abnormalities include angiokeratoma corporis diffusum, widespread telangiectasia, thick skin, hyperhidrosis and hypohidrosis, acrocyanosis and distal transverse nail bands. It has been described that >50% of fucosidosis patients have angiokeratoma. At molecular level, fucosidosis is caused by lysosomal alpha-L-fucosidase (FUCA1) gene mutations. Obtaining samples for functional studies has been challenging due to the inherent difficulty in finding affected individuals. The effect of *FUCA1* dysfunction on gene expression is unknown.

The aim of the present study was to analyse, in keratinocytes, the transcriptomic effect of *FUCA1* knock-down for a better understanding of skin lesions' pathogenesis affecting fucosidosis patients. *FUCA1* knock-down (siRNA) was performed in human HaCaT immortalised keratinocytes. Affymetrix arrays and qPCR were used for analysing gene expression. Bioinformatics was used for functional clustering of modified genes.

387 genes showed differential expression between *FUCA1* silenced and non-silenced cells (222 up-regulated and 165 down-regulated). Upregulated genes belonged to two major groups: keratinocyte differentiation/epidermal development (n=17) and immune response (n= 61). Several transcription factors were upregulated in *FUCA1*-siRNA transfected cells. This effect might partly have been produced by abnormal transcription factor expression, i.e. *FOXN1*. We thus propose that fucosidosis-related skin lesions (e.g. angiokeratoma) and those of other diseases (e.g. psoriasis) might be caused by dysfunctions in common aetiological overlapping molecular cascades.

Keywords: Transcriptome; lysosomal alpha-L-fucosidase; angiokeratoma; *FOXN1*; skin disease.

Introduction

Fucosidosis is a rare lysosomal storage disease which is inherited as an autosomal recessive trait. It is mainly characterised by progressive intellectual disability, delayed development of motor skills, retarded growth, frequent infections, dysostosis multiplex, coarse facial features, angiokeratoma, visceromegaly and seizures (1). Fucosidosis has been classified into two subtypes, depending on the severity of clinical signs and symptoms. Type 1 has been reported as having a severe infantile presentation (neurological functions being highly affected before 1 year of age) while type 2 has progressive features, increasing patient's life expectancy to 25-35 years of age (2). Fucosidosis patients' skin abnormalities include angiokeratoma corporis diffusum (which is also present in other metabolic diseases), widespread telangiectasia, skin thickness, hyperhidrosis and hypohidrosis, acrocyanosis and distal transverse nail bands (1, 3-5). It has been described that >50% of fucosidosis patients have angiokeratoma which tends to spread over the body of older patients; such lesions, located in the papillary dermis, are characterised by proliferative ectatic blood vessels limited by a flattened endothelium containing erythrocytes (6). Affected cells, including keratinocytes, have cytoplasmic vacuoles containing a membranous or granular substance.

At molecular level, fucosidosis is caused by lysosomal alpha-L-fucosidase (*FUCA1*) gene mutations encoding the α-L-fucosidase enzyme responsible for fucose hydrolysis (1, 7). *FUCA1* biallelic mutations (point mutations, deletions and insertions) lead to an abnormal accumulation of glycopeptides, fucosyl-glycolipids and oligosaccharides in distinct tissues.

Only a few *FUCA1* mutations have been described to date and some genotype-phenotype correlations have been proposed (8).

Obtaining samples for functional studies has been challenging due to the inherent difficulty in finding affected individuals. A knock-out mouse model of *Fuca1* had lysosomal storage pathology affecting visceral organs such as the central nervous system, bladder, spleen and liver but was not affected by skin dysfunction (9).

The present study analysed, in keratinocytes, the transcriptomic effect of *FUCA1* knockdown for a better understanding of skin lesions' pathogenesis affecting fucosidosis patients.

We found expression disturbances regarding genes mainly related to keratinocyte differentiation/epidermal development and immune responses. Interestingly, we identified the abnormal expression of some transcription factors. *FOXN1* underlined a particular interest, as it has been clearly involved in the regulation of several skin keratinocytes´ molecular pathways. In addition, *Foxn1* mutant mice displayed abnormal skin phenotypes, some of which resemble to those observed in human disease.

We propose that fucosidosis-related skin lesions (e.g. angiokeratoma) and those related to other diseases (e.g. psoriasis) might be caused by dysfunctions in commonly occurring aetiological overlapping molecular cascades.

Methods

Cell culture and *FUCA1* siRNA transfection

Dr Isabel Ortiz (Universidad Pontificia Bolivariana, Bogotá, Colombia) kindly provided the human HaCaT immortalised keratinocyte cell line. Cells were cultured in Dulbecco's modified Eagle medium/Ham's Nutrient Mixture F12 (DMEM/F12, Gibco) containing 10% foetal bovine serum (FBS-Biowest) and 1% penicillin/streptomycin (Invitrogen-Gibco, Carlsbad, CA, U.S.A) at 37°C in a 5% CO_2 atmosphere. Transfection assays were divided into two groups: control cells transfected with scrambled sequence siRNA-A (NTC) (Santa Cruz Biotechnology, Inc, sc 37007), and transfected cells (TSC) with *FUCA1*-targeting siRNA (sc 78583) (Santa Cruz Biotechnology, Santa Cruz, CA, U.S.A). Cells were seeded in four wells (200,000 cells/well) on 6-well plates and incubated at 37°C for 24 hours for each condition (NTC, TSC). TSC and NTC groups were transfected with 80 pmol/well of specific siRNA, according to the manufacturer´s recommendations. Two biological replicates of TSC and NTC groups were performed. Sixty hours thereafter, TCS and NTC were harvested for total RNA extraction.

RNA extraction and *FUCA1* RT-PCR

An Ambion Purelink RNA mini kit (Invitrogen) was used for extracting total RNA from NTC (4 wells) and TSC (4 wells). RNA amount and quality were verified with the Bioanalyzer 2100 (version 2.6) (Agilent, Santa Clara, CA, EE.UU) and by electrophoresis. The SuperScript III First-Strand Synthesis System (Invitrogen) with oligo [dT] primers was then used for reverse transcribing RNA to cDNA, following the manufacturer's instructions. 100 ng of cDNA and commercial primers (sc78583) (Santa Cruz Biotechnology) were used for RT-PCR. RT-PCR consisted of one denaturation step at 94°C (10 minutes), followed by 30 cycles at 94°C (40 seconds), 58°C (40 seconds), 72°C (40 seconds) an a final step of 72°C (10 minutes).

Gene expression studies using Affymetrix microarrays

Affymetrix's GeneChip Primeview human gene expression arrays (Thermo Fisher, Waltham, MA. Ref. 901837) were used for analysing RNA extracted from TSC and NTC. Six distinct microarrays were used for TSC and NTC (technical replicates). The robust multi-array average (RMA) algorithm was used for data normalisation and summarising. Data were log2 transformed and expression levels were subtracted between conditions (TSC–NTC). Values <1 and >1 were representative of two-fold expression changes (up- and down-regulation, respectively) and were considered to be biologically relevant. The Institute for Research in Biomedicine's (IRB**,** Barcelona, Spain**)** Functional Genomics Core (FGC) performed the transcriptomics assays.

Real-Time Quantitative PCR (qPCR) assay

TSC or NTC retrotranscribed cDNA (20ng) was used for each qPCR reaction (*FUCA1*, *KRT4*, *KRT1*, *KRT16*, *TGM1*, *EDAR*, *S100A7*, *OVOL1*, *SCEL*, *SPRR2A*, *SPRR2D*, *IRF9*, *IRF1*, *GBP2*, *ICAM1*, *IFI27*). Primer sequences were obtained from the Primer Bank Database (http://pga.mgh.harvard.edu/primerbank/) (**Supplementary Table S1**).

SYBR Green PCR Master Mix (Thermo Fisher Scientific) was used for qPCR experiments, involving a QuantStudio 3 Real-Time PCR system (Thermo Fisher Scientific). For PCRs reaction we used: 20 ng/µl of cDNA, 1X SYBR Green PCR Master Mix (Applied Biosystems, Foster City, CA, U.S.A), 0.4 µM of each primer and ultrapure water (final volume 20 µl). The qPCR was performed with the following conditions: an initial enzyme activation step at 95°C (10 minutes), followed by 40 cycles at 95°C (30 seconds), 61°C (30 seconds) and 72°C (25 seconds) (signal acquisition). A melting curve analysis was used for verifying primer specificity and primer-dimer potential formation. The standard curve method was used for expression analysis

Statistical analysis and bioinformatics

FUCA1 differential expression levels between NTC and TSC were calculated from the .CEL files using R 3.0.0 software (www.r-project.org). The moderated t-statistic test was used for establishing statistically significant expression differences between conditions (NTC *vs* TSC) in the microarray experiments. Statistical analysis was completed with SPSS software (version 24, SPSS Inc.). DAVID software (https://david.ncifcrf.gov/) was used for gene ontology analysis. Functional clusters were generated for up- and down-regulated genes in an independent manner, as previously recommended (10). Statistical difference was assessed using the two-sided t-Student test for calculate significant expression differences between conditions in the qPCR experiments.

Results

TSC *FUCA1* RT-PCR bands had considerably less intensity than those from NTC (**Supplementary Figure S1**). In the microarray, the *FUCA1* average expression levels (in terms of fluorescence) for NTC and TSC were 7.24 and 6.123 respectively ($p=1.93x10^{-6}$) (**Supplementary Table S2**). NTC *FUCA1* qPCR expression levels compared to those for TSC had statistically significant differences ($2.36x10^{10}$ *vs* $2.37x10^{11}$ copies, respectively; $p=2.04\ x10^{-7}$). Expression microarrays revealed that 387 genes were dysregulated between NTC and TSC (222 up-regulated and 165 down-regulated) (**Supplementary Tables S2**). Bioinformatics clustering of up-regulated genes revealed 12 functional categories involving different biological processes. Manually reorganising this data (due to overlapping categories) led to identifying two major groups: keratinocyte differentiation/epidermal development (n=17) and immune response (n= 61) (**Figure 1, Supplementary Figure S2**). No functional clustering could be established for downregulated genes. All the differential expressed genes tested by qPCR revealed identical behaviour (up- or down-regulation) to that observed in the microarray assays (**Supplementary Figure S3, Supplementary Table S2**).

Discussion

The present work was aimed at identifying keratinocyte gene expression disturbances at transcriptomic level caused by *FUCA1* down-regulation. Although most *FUCA1* mutations encountered in fucosidosis patients lead to drastically low fucosidase enzyme activity, we adopted a conservative gene knock-down strategy (rather than a complete knock-out approach) to avoid potentially strong cell damage and identify representative molecular actors in the disease's pathogenesis. We consider that microarray data expression profiles were robust since six technical replicates (from two biological replicates) were performed for NTC and TSC conditions. Furthermore, qPCR experiments performed for several genes displaying differential expression confirmed up- or down-regulation gene expression reported from our microarray experiments.

FUCA1 knock-down in keratinocytes led to the overexpression of genes involved in two key skin physiology-related biological processes: keratinocyte differentiation/epidermal development and immune response (**Figure 1, Supplementary Figure S2**). Functional gene clustering was performed by using DAVID software, which has been widely used for classifying genes based by measuring gene-gene similarity. The method is based on the assumption that genes sharing overall functional annotation profiles are functionally related to each other. This software also has an agglomeration method for grouping related genes (or terms) into functional groups (biological modules) (11, 12). Functional groups are then ranked, based on all group members' overall participation in the enriched biological processes associated with the total gene list. *KRT16* and *S100A7* were identified in these categories' intersection, arguing in favour of their functional relevance and potential interactions regarding skin lesion pathogenesis observed in fucosidosis patients. To note, DAVID clustering has stringent parameters for establishing genes'

individual functional categories. A gene being present in various categories may therefore signify that it performs important roles during/involved in different biological processes.

KRT16 belongs to the large keratin-encoding gene family which is highly expressed in keratinocytes, performing essential skin biology functions (13). Keratins form intermediate filaments, a complex dynamic cytoskeleton structure providing tissue stability, mechanical integrity and flexibility. *S100A7* encodes psoriasin, a protein having multiple functions such as calcium homeostasis regulation, cell differentiation/proliferation, apoptosis, cytoskeleton function, inflammation and immune response (14). Keratins (e.g. KRT6,-16, -17) and molecules related to damage-associated molecular patterns (S100 proteins, some chemokines and cytokines) are overexpressed secondary to keratinocytes' stress conditions which have been linked to several diseases' pathophysiology (15-18). Interestingly, several other genes (e.g. *SPRRs*, *CRABP2*, *KRT1*, *KRT4*, *TGM1*) which were overexpressed in our study have also been shown to have up-regulation patterns in different pathological conditions displaying hyperkeratosis, thereby arguing in favour of common molecular mechanisms (19-22). Gene functional clustering revealed that a considerable percentage of genes belonged to immunological and inflammatory molecular pathways; this finding is particularly interesting, since several molecules (e.g. cytokines, chemokines, alarmins, HLAs) had similar behaviour in mouse models of diseases involving immune response mechanisms, such as psoriasis (22, 23).

Among the overexpressed functionally-clustered molecules, FOXN1, STAT2, TXNIP, OVOL1, IRF1, IRF7, IRF9 and SP100 proteins have transcriptional regulation properties. FOXN1, a protein belonging to the forkhead box family of transcription factors, has been defined as being a key molecule regulating thymic epithelial cells and skin keratinocytes (24, 25). Mutant *Foxn1* has been associated with thymic dysgenesis and has led to a hairless phenotype (Nude) in mice and humans

(26, 27). *Foxn1* overexpression in mice led to increased skin permeability and similar, but less severe, structural changes to those seen in congenital ichthyosis (28, 29). Epidermal thickening in *Foxn1* deficient (nude) mice has been associated with various changes in the skin's lipid profile (lipidome), such as an increase in cholesterol sulphate which, in turn, might be related to increased abundance of filaggrin (FLG) (30). Our results highlighted FLG down-regulation which might have been caused by FOXN1 up-regulation, secondary to *FUCA1* knock-down. Although FOXN1 direct and indirect gene targets have not been completely elucidated, it has been shown that it can regulate Notch ligands, chemokines and matrix metalloproteinase molecules (31-34). *FOXN1* up-regulation could thus have contributed to the considerable amount of expression disturbances (up- and down-regulation) found in our study, including those observed in this kind of molecules (e.g. *CCL22*, *MMP7*). These findings argue in favour of a central role for *FOXN1* in the pathophysiology of skin lesions found in fucosidosis patients. To note, our experimental approach did not prove directly that FOXN1 was responsible for downstream regulation of genes differentially expressed in *FUCA1* silenced cells. Chromatin immunoprecipitation sequencing (ChIP-Seq) experiments could be performed to identify downstream direct FOXN1 targets; transcriptomic analysis of whether cells are overexpressing (e.g. FOXN1-WT version transfections) or not *FOXN1* (mock transfection) could be done using microarrays to assess potential direct and indirect downstream targets.

Similarly to FOXN1, STAT2, OVOL1 and IRF9, which were overexpressed in TSC cells, might contribute to the phenotype, as they have been shown to have relevant functions in skin disease development (35-40).

Concerning our down-regulated gene clustering annotation, it is worth noting that we could not establish functional categories. This was probably due to the small amount (n=165) of down-regulated genes, in turn resulting from our conservative *FUCA1* down-regulation strategy. However, manual checking of data revealed a relevant amount of down-regulated genes linked to skin physiology (e.g. *FLG*, *GJA1*, *CALB2*, *TNC*, *CBS*, *THBS1*).

Taken together, our results have shown that *FUCA1* down-regulation leads to expression disturbances regarding genes mainly related to keratinocyte differentiation/epidermal development and immune responses. This effect might partly have been produced by abnormal transcription factor expression, i.e. *FOXN1*. We thus hypothesize that fucosidosisrelated skin lesions (e.g. angiokeratoma) and those of other diseases (e.g. psoriasis) might be caused by dysfunctions in common aetiological overlapping molecular cascades.

Acknowledgments

DV, KMJ, CP and DJF performed the research and analysed the data. PL designed the research study, analysed the data and wrote the paper. All authors worked on and approved the final version of the manuscript. We would like to acknowledge the Functional Genomic Core (IRB, Barcelona, Spain) which performed the microarray experiments.

Conflict of interest

The authors declare no conflict of interest.

References

1. Willems P J, Gatti R, Darby J K, et al. Fucosidosis revisited: a review of 77 patients. American journal of medical genetics 1991: 38: 111-131.
2. Michalski J C, Klein A. Glycoprotein lysosomal storage disorders: alpha- and betamannosidosis, fucosidosis and alpha-N-acetylgalactosaminidase deficiency. Biochimica et biophysica acta 1999: 1455: 69-84.
3. George S, Graham-Brown R A. Angiokeratoma corporis diffusum in fucosidosis. Journal of the Royal Society of Medicine 1994: 87: 707.
4. Fleming C, Rennie A, Fallowfield M, et al. Cutaneous manifestations of fucosidosis. The British journal of dermatology 1997: 136: 594-597.
5. Tsukadaira A, Hirose Y, Aoki H, et al. Diagnosis of fucosidosis through a skin rash. Internal medicine 2005: 44: 907-908.
6. Kanitakis J, Allombert C, Doebelin B, et al. Fucosidosis with angiokeratoma. Immunohistochemical & electronmicroscopic study of a new case and literature review. Journal of cutaneous pathology 2005: 32: 506-511.
7. Patel V, Watanabe I, Zeman W. Deficiency of alpha-L-fucosidase. Science 1972: 176: 426-427.
8. Akagi M, Inui K, Nishigaki T, et al. Mutation analysis of a Japanese patient with fucosidosis. Journal of human genetics 1999: 44: 323-326.
9. Wolf H, Damme M, Stroobants S, et al. A mouse model for fucosidosis recapitulates storage pathology and neurological features of the milder form of the human disease. Disease models & mechanisms 2016: 9: 1015-1028.
10. Hong G, Zhang W, Li H, et al. Separate enrichment analysis of pathways for up- and downregulated genes. Journal of the Royal Society, Interface 2014: 11: 20130950.

11. Huang D W, Sherman B T, Tan Q, et al. The DAVID Gene Functional Classification Tool: a novel biological module-centric algorithm to functionally analyze large gene lists. Genome biology 2007: 8: R183.

12. Huang da W, Sherman B T, Lempicki R A. Systematic and integrative analysis of large gene lists using DAVID bioinformatics resources. Nature protocols 2009: 4: 44-57.

13. Moll R, Divo M, Langbein L. The human keratins: biology and pathology. Histochemistry and cell biology 2008: 129: 705-733.

14. Jia J, Duan Q, Guo J, et al. Psoriasin, a multifunctional player in different diseases. Current protein & peptide science 2014: 15: 836-842.

15. DePianto D, Coulombe P A. Intermediate filaments and tissue repair. Experimental cell research 2004: 301: 68-76.

16. Nestle F O, Di Meglio P, Qin J Z, et al. Skin immune sentinels in health and disease. Nature reviews Immunology 2009: 9: 679-691.

17. Lessard J C, Pina-Paz S, Rotty J D, et al. Keratin 16 regulates innate immunity in response to epidermal barrier breach. Proceedings of the National Academy of Sciences of the United States of America 2013: 110: 19537-19542.

18. Cubillos S, Norgauer J. Low vitamin D-modulated calcium-regulating proteins in psoriasis vulgaris plaques: S100A7 overexpression depends on joint involvement. International journal of molecular medicine 2016: 38: 1083-1092.

19. Chamcheu J C, Siddiqui I A, Syed D N, et al. Keratin gene mutations in disorders of human skin and its appendages. Archives of biochemistry and biophysics 2011: 508: 123137.

20. Schafer M, Willrodt A H, Kurinna S, et al. Activation of Nrf2 in keratinocytes causes chloracne (MADISH)-like skin disease in mice. EMBO molecular medicine 2014: 6: 442-457.

21. Ortega-Recalde O, Moreno M B, Vergara J I, et al. A novel TGM1 mutation, leading to multiple splicing rearrangements, is associated with autosomal recessive congenital ichthyosis. Clinical and experimental dermatology 2015: 40: 757-760.

22. Lundberg K C, Fritz Y, Johnston A, et al. Proteomics of skin proteins in psoriasis: from discovery and verification in a mouse model to confirmation in humans. Molecular & cellular proteomics : MCP 2015: 14: 109-119.

23. Swindell W R, Johnston A, Carbajal S, et al. Genome-wide expression profiling of five mouse models identifies similarities and differences with human psoriasis. PloS one 2011: 6: e18266.

24. Gawronska-Kozak B, Grabowska A, Kopcewicz M, et al. Animal models of skin regeneration. Reproductive biology 2014: 14: 61-67.

25. Zhang Z, Burnley P, Coder B, et al. Insights on FoxN1 biological significance and usages of the "nude" mouse in studies of T-lymphopoiesis. International journal of biological sciences 2012: 8: 1156-1167.

26. Nehls M, Pfeifer D, Schorpp M, et al. New member of the winged-helix protein family disrupted in mouse and rat nude mutations. Nature 1994: 372: 103-107.

27. Mecklenburg L, Tychsen B, Paus R. Learning from nudity: lessons from the nude phenotype. Experimental dermatology 2005: 14: 797-810.

28. Mandinova A, Kolev V, Neel V, et al. A positive FGFR3/FOXN1 feedback loop underlies benign skin keratosis versus squamous cell carcinoma formation in humans. The Journal of clinical investigation 2009: 119: 3127-3137.

29. Ruan L, Zhang Z, Mu L, et al. Biological significance of FoxN1 gain-of-function mutations during T and B lymphopoiesis in juvenile mice. Cell death & disease 2014: 5: e1457.

30. Lanzini J, Dargere D, Regazzetti A, et al. Changing in lipid profile induced by the mutation of Foxn1 gene: A lipidomic analysis of Nude mice skin. Biochimie 2015: 118: 234243.

31. Bleul C C, Boehm T. Chemokines define distinct microenvironments in the developing thymus. European journal of immunology 2000: 30: 3371-3379.

32. Tsukamoto N, Itoi M, Nishikawa M, et al. Lack of Delta like 1 and 4 expressions in nude thymus anlages. Cellular immunology 2005: 234: 77-80.

33. Gawronska-Kozak B. Scarless skin wound healing in FOXN1 deficient (nude) mice is associated with distinctive matrix metalloproteinase expression. Matrix biology : journal of the International Society for Matrix Biology 2011: 30: 290-300.

34. Palamaro L, Romano R, Fusco A, et al. FOXN1 in organ development and human diseases. International reviews of immunology 2014: 33: 83-93.

35. Gamero A M, Young M R, Mentor-Marcel R, et al. STAT2 contributes to promotion of colorectal and skin carcinogenesis. Cancer prevention research 2010: 3: 495-504.

36. Neumann C, Bigliardi-Qi M, Widmann C, et al. The delta-opioid receptor affects epidermal homeostasis via ERK-dependent inhibition of transcription factor POU2F3. The Journal of investigative dermatology 2015: 135: 471-480.

37. Tsuji G, Hashimoto-Hachiya A, Kiyomatsu-Oda M, et al. Aryl hydrocarbon receptor activation restores filaggrin expression via OVOL1 in atopic dermatitis. Cell death & disease 2017: 8: e2931.

38. Ito T, Tsuji G, Ohno F, et al. Potential role of the OVOL1-OVOL2 axis and c-Myc in the progression of cutaneous squamous cell carcinoma. Modern pathology : an official journal of the United States and Canadian Academy of Pathology, Inc 2017: 30: 919-927.

39. Johansen C, Rittig A H, Mose M, et al. STAT2 is involved in the pathogenesis of psoriasis by promoting CXCL11 and CCL5 production by keratinocytes. PloS one 2017: 12: e0176994.

40. Zolotarenko A, Chekalin E, Mehta R, et al. Identification of Transcriptional Regulators of Psoriasis from RNA-Seq Experiments. Methods in molecular biology 2017: 1613: 355-370.

Figure Legends

Figure 1. Heat map schemes showing differential gene expression between control and FUCA1 silenced cells. **(a)** Genes belonging to immune response biological processes **(b)** Genes belonging to keratinocyte differentiation/epidermal development biological processes. TSC: transfected cells with *FUCA1*-targeting siRNA. NTC: cells transfected with scrambled sequence siRNA-A (negative control).

Supplementary Figure S1. *FUCA1* Knock-down. **(a)** RT-PCR experiments, **(b)** qPCR experiments *** p-value <0.001. TSC: transfected cells with *FUCA1*-targeting siRNA. NTC: cells transfected with scrambled sequence siRNA-A (negative control). L: Ladder

Supplementary Figure S2. Functional clustering of up regulated genes.

Supplementary Figure S3: qPCR of 16 genes ** p-value <0.01 *** p-value <0.001. TSC: transfected cells with *FUCA1*-targeting siRNA. NTC: cells transfected with scrambled sequence siRNA-A (negative control).

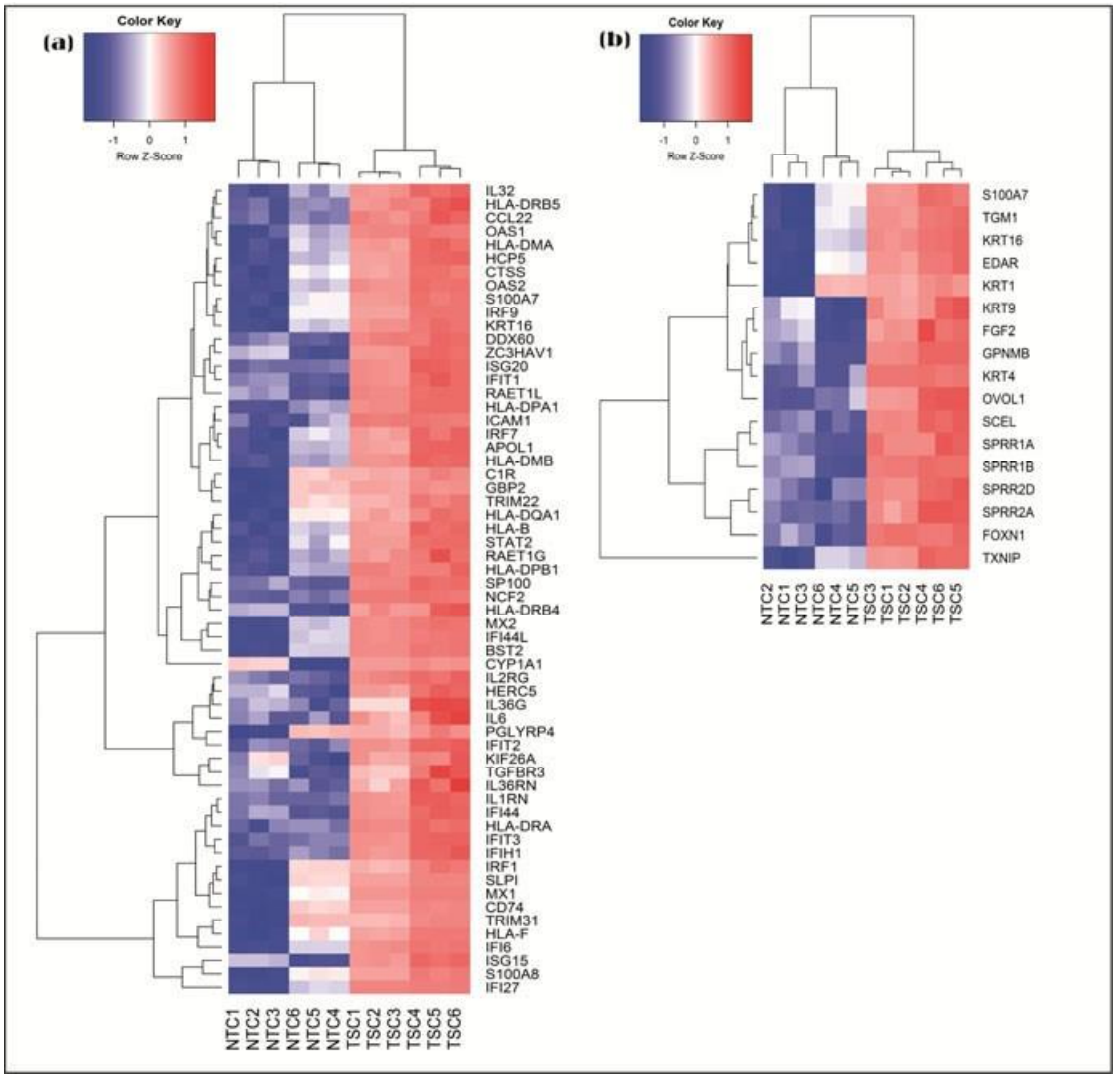

Anexo 2: Tabla de los genes desregulados en el microarreglo.

Genes sobre expresados en el microarreglo

Gene symbol	Gene name	Probe	Fold Change	Adj. p.Val
SPRR1B	Small proline rich protein 1B	11725369_at	10,675271	2,27E-07
BST2	Bone marrow stromal cell antigen 2	11716034_a_at	9,47836912	4,12E-05
		11716036_x_at	8,18212389	1,61E-05
		11716035_at	7,93054152	6,37E-06
IFI27	Interferon alpha inducible protein 27	11715893_s_at	8,5760124	6,89E-05
		11757480_x_at	6,46439018	3,64E-04
IFI44L	Interferon induced protein 44 like	11723234_at	8,15458368	5,17E-05
		11723235_a_at	6,81502682	1,81E-06
		11723236_at	3,24906839	6,61E-07
NDUFS2	NADH: ubiquinone oxido reductase core subunit S2	11760705_a_at	6,12058564	2,78E-08
SPRR1A	Small proline rich protein 1A	11730911_at	5,86946365	7,32E-08

		11754180_s_at	3,06966702	5,63E-09
LY6G6C	Lymphocyte antigen 6 complex, locus G6C	11729478_at	5,79032709	4,25E-09
		11729477_a_at	2,00645262	1,61E-05
IFI6	Interferon alpha inducible protein 6	11718986_a_at	5,76653273	6,55E-05
S100P	S100 calcium binding protein P	11718347_a_at	5,45328621	1,89E-03
ERP27	Endoplasmic reticulum protein 27	11723627_at	5,30686656	2,21E-06
MX2	MX dynamin like GTPase 2	11726479_a_at	5,27950663	2,77E-05
		11753064_a_at	3,01938662	1,70E-05
ATP6V0D2	ATPaseH + transporting V0 subunit D2	11735046_at	4,72484155	3,01E-10
CYP1A1	Cytochrome P450 family 1 subfamily A member 1	11726536_at	4,64863466	9,00E-03
		11754154_a_at	4,24801161	1,24E-02
C15orf48	Chromosome 15 open reading frame 48	11743350_a_at	4,62543992	1,35E-03
SCEL	Sciellin	11746764_a_at	4,6199348	4,37E-09
		11746765_x_at	3,89975116	1,95E-08
		11748044_a_at	3,72336968	3,01E-10
		11734853_x_at	3,30002525	3,54E-10
		11738827_a_at	2,82645885	7,05E-08

		11744607_at	2,490919	7,52E-07
B3GNT7	UDP-GlcNAc: beta Gal beta-1,3-N-acetyl glucosaminyltransferase 7	11729998_a_at	4,59898886	4,38E-05
		11729999_a_at	2,98773369	1,20E-06
FAM25BP	Protein FAM 25	11758699_x_at	4,55925638	8,56E-10
SERPINB3	Serpin family B member 3	11752804_a_at	4,5521188	1,16E-02
		11752806_x_at	4,16660685	7,14E-03
		11752805_s_at	3,98770338	5,81E-03
		11729694_s_at	3,75769213	1,07E-02
		11753202_s_at	3,65736342	1,13E-02
		11729692_a_at	3,44703578	5,60E-03
		11729693_at	3,32973493	6,07E-03
		11753201_a_at	3,11185648	3,75E-02
		11730263_x_at	2,6314268	1,12E-02
INSIG1	Insulin induced gene 1	11716339_a_at	4,19504369	1,46E-04
		11716338_a_at	4,01089066	8,01E-05
		11716337_s_at	3,81497126	4,76E-04
RAET1L	Retinoic acid early transcript 1L	11738222_x_at	4,18363727	3,11E-07

		11726551_s_at	2,41841665	2,14E-07
		11745700_s_at	2,27408422	7,35E-10
SLC39A2	Solute carrier family 39 member 2	11728506_at	3,80825997	3,76E-03
CACNG6	Calcium voltage-gated channel auxiliary subunit gamma 6	11742124_a_at	3,80474738	1,45E-09
KRT16	Keratin 16	11748328_s_at	3,43264322	4,98E-05
KRT1	Keratin 1	11723952_at	3,38158432	2,05E-02
TJP2	Tight junction protein 2	11763304_at	3,38107392	1,23E-06
KLK13	Kallikrein related peptidase 13	11737031_a_at	3,38065929	8,89E-08
		11750242_a_at	2,8686098	2,05E-05
ACE2	Angiotensin converting enzyme 2	11725625_s_at	3,37115996	6,23E-07
		11725624_at	2,91895782	4,25E-06
		11725626_a_at	2,89834734	1,46E-07
HLA-B	Major histocompatibility complex, classI, B	11762851_at	3,36732362	1,22E-05
KLK11	Kallikrein related peptidase 11	11729069_a_at	3,3360519	5,80E-05
PSAPL1	Prosaposin-like1 (gene/pseudogene)	11740428_at	3,22040684	2,06E-10
TMEM37	Transmembrane protein 37	11754171_a_at	3,16423777	1,09E-02
HLA-DPB1	Major histocompatibility complex, classII, DP beta1	11756073_x_at	3,11449455	3,16E-06

		11757801_x_at	2,49794655	1,43E-05
		11760799_x_at	2,2859468	2,49E-06
NCF2	Neutrophil cytosolic factor 2	11741153_a_at	3,07452926	3,54E-10
TGM1	Transglutaminase 1	11741819_a_at	3,04819183	2,76E-04
GPNMB	Glycoprotein NMB	11759826_x_at	2,98365996	1,46E-07
		11740089_x_at	2,97655608	5,80E-04
		11742871_a_at	2,96819742	3,39E-04
		11757868_a_at	2,95598296	9,76E-05
		11751393_a_at	2,89459263	2,92E-04
		11742872_s_at	2,39477226	8,65E-04
		11751394_s_at	2,32824813	6,73E-04
PIK3IP1	Phosphoinositide-3-kinase interacting protein 1	11740088_s_at	2,13410769	3,85E-06
		11736661_a_at	2,97308529	1,11E-02
MAP3K13	Mitogen-activated protein kinase kinase13	11747248_a_at	2,30059972	1,89E-02
		11731706_at	2,95319626	2,57E-08
CCL22	C-Cmotif chemokine ligand 22	11731705_at	2,13451675	6,47E-08
PI3	Peptidase inhibitor 3	11721650_at	2,94219941	4,69E-07

NDRG4	NDRG family member 4	11736068_x_at	2,9297572	3,18E-05
		11743415_s_at	2,52825966	2,56E-06
YPEL3	Yippee like 3	11721356_s_at	2,92651597	1,87E-05
		11726780_x_at	2,91331111	2,45E-05
		11721355_a_at	2,64529195	7,12E-05
KLHL24	Kelch lik efamily member 24	11756440_a_at	2,92166757	2,06E-10
		11757390_s_at	2,73476125	9,72E-06
		11729691_a_at	2,72565466	9,63E-07
HERC5	HECT and RLD domain containing E3 ubiquitin protein ligase 5	11755374_a_at	2,9182749	1,49E-05
OAS2	2'-5'-oligo adenylate synthetase 2	11736135_at	2,90388516	1,86E-05
		11726201_a_at	2,65715706	2,18E-05
		11736136_s_at	2,34685503	1,19E-05
		11736134_a_at	2,3246288	1,81E-04
CDH23	Cadherin related 23	11735501_a_at	2,89443267	8,27E-08
HLA-DRA	Major histocompatibility complex, classII, DR alpha	11742850_x_at	2,85702442	5,44E-08
		11744484_s_at	2,7656854	1,44E-08
CAPN5	Calpain 5	11718753_a_at	2,84509556	1,35E-07

IL36G	Interleukin 36, gamma	11753008_a_at	2,82076746	3,12E-07
PDK4	Pyruvate dehydrogenase kinase 4	11716975_a_at	2,81592034	1,88E-03
		11716974_a_at	2,50755767	1,16E-03
GBP2	Guanylate binding protein 2	11719447_s_at	2,81038026	1,33E-02
HLA-DPA1	Major histocompatibility complex, classII, DP alpha 1	11715583_s_at	2,79915561	2,76E-07
		11758231_x_at	2,79061524	5,84E-08
IRF9	Interferon regulatory factor 9	11720208_a_at	2,79520375	3,94E-04
		11746156_x_at	2,48357677	4,86E-04
		11720209_at	2,37725363	2,16E-03
		11746155_a_at	2,26951081	2,74E-04
IDO1	Indoleamine 2,3-dioxygenase 1	11743168_at	2,7736584	1,03E-02
MXD1	MAX dimerization protein 1	11719249_at	2,76660684	5,47E-04
		11750016_a_at	2,52128519	1,25E-04
DDX60	DExD/H-boxhelicase60	11744236_a_at	2,75028116	1,66E-08
HLA-DQA1	Major histocompatibility complex, classII, DQ alpha1	11753898_x_at	2,74818423	1,39E-03
		11724799_x_at	2,64518186	5,40E-04
		11750527_s_at	2,37737308	1,75E-08

		11721615_a_at	2,72598502	2,25E-04
		11763675_at	2,71877661	1,20E-04
		11752610_a_at	2,24812481	1,23E-06
THEMIS2	Thymocyte selection associated family member 2	11721617_x_at	2,02606079	2,04E-05
ATP6V1B1	ATPase H+transporting V1 subunit B1	11718919_a_at	2,71513673	2,92E-02
		11737477_a_at	2,71302577	8,66E-03
C2orf54	Chromosome 2 ope nreading frame 54	11745353_a_at	2,41725004	2,48E-03
S100A7A	S100 calcium binding protein A7A	11725459_s_at	2,71293033	7,72E-04
RTP4	Receptor transporter protein 4	11725240_at	2,70323652	1,01E-03
UPK3B	Uroplakin 3B	11730326_x_at	2,69437401	2,36E-09
		11720007_a_at	2,68676866	4,07E-03
		11750736_a_at	2,3549827	7,78E-03
STEAP4	STEAP4 metalloreductase	11720008_a_at	2,1461496	6,51E-04
GCNT3	Glucosaminyl(N-acetyl) transferase3, mucintype	11724528_a_at	2,68569001	5,63E-09
		11729713_x_at	2,67957953	1,57E-10
SPRR2A	Small proline rich protein 2A	11729712_at	2,34412721	4,09E-10
CLIC5	Chloride intracellular channe l5	11732372_a_at	2,67713397	9,59E-08

		11755748_s_at	2,66291223	5,54E-04
		11739482_x_at	2,32184308	3,29E-03
		11755747_a_at	2,22665081	4,75E-04
PLAC8	Placenta specific 8	11720867_x_at	2,02806678	2,08E-04
IFIT1	Interferon induced protein with tetratricopeptide repeats 1	11756820_a_at	2,65953385	1,38E-08
PKD1L2	Polycystin 1like 2 (gene/pseudogene)	11734387_at	2,65781674	1,73E-07
		11753882_a_at	2,63178743	4,37E-09
		11720207_a_at	2,24112217	2,68E-09
		11753883_x_at	2,18761485	5,63E-09
IL2RG	Interleukin 2 receptor subunit gamma	11753814_a_at	2,09041454	2,49E-06
CXorf49	Chromosome X open reading frame 49	11738259_s_at	2,62665338	5,51E-05
		11741012_a_at	2,62662257	2,06E-10
		11757764_s_at	2,54151241	1,60E-09
MSMO1	Methyl sterol monooxygenase 1	11740092_x_at	2,53715893	4,58E-08
S100A7	S100 calcium binding protein A7	11725460_x_at	2,61599459	4,13E-04
		11723989_s_at	2,6097459	5,55E-08
THRA	Thyroid hormone receptor, alpha	11747681_x_at	2,51462885	9,72E-08

TNS1	Tensin 1	11716559_x_at	2,60676611	8,44E-04
		11716558_at	2,38205464	1,34E-04
GADD45B	Growth arrest and DNA damage inducible beta	11757865_a_at	2,60408218	3,21E-10
		11759525_at	2,23566935	3,03E-09
		11764031_at	2,1344542	6,52E-08
EDAR	Ectodysplasin A receptor	11733559_a_at	2,59193174	5,78E-04
		11751007_a_at	2,14553287	6,53E-04
CD74	CD74 molecule	11726255_x_at	2,59147147	6,01E-03
		11739401_a_at	2,50020356	8,48E-03
		11738435_x_at	2,38924796	4,96E-03
		11756766_x_at	2,37554227	5,54E-03
		11726254_s_at	2,35379794	3,75E-03
ALDH3B2	Aldehyde dehydrogenase 3 family member B2	11727500_at	2,58143573	1,09E-02
KRT4	Keratin 4	11739440_a_at	2,57666206	4,37E-08
TGFBR3	Transforming growth factor beta receptor 3	11718901_at	2,57575005	2,53E-05
ZC3HAV1	Zinc finger CCCH-type containing, antiviral 1	11756839_x_at	2,53522382	1,16E-05
TSC22D3	TSC22 domain family member 3	11751415_a_at	2,51796971	6,26E-05

		11717829_s_at	2,33742531	7,32E-05
		11717830_a_at	2,24426455	3,86E-04
OAS1	2'-5'-oligoadenylate synthetase 1	11724256_s_at	2,51256768	1,63E-05
		11724255_a_at	2,43063149	2,08E-06
		11740891_a_at	2,2388498	2,44E-06
		11719588_a_at	2,11881164	8,68E-05
TRIM22	Tripartite motif containing 22	11722368_a_at	2,50811462	3,43E-03
		11755587_a_at	2,41051731	5,97E-03
		11722369_x_at	2,35800923	5,38E-03
		11750170_a_at	2,00670948	1,11E-02
GSDMB	Gasdermin B	11726557_a_at	2,49957997	1,86E-02
RNASE4	Ribonuclease A family member 4	11718988_s_at	2,49857026	1,88E-06
ECM1	Extracellular matrix protein 1	11748525_a_at	2,49649529	4,11E-05
		11717891_a_at	2,34872421	1,18E-05
CLIC3	Chloride intracellular channel 3	11724885_at	2,49067965	2,69E-03
MFSD4A	Major facilitator superfamily domain containing 4A	11746475_a_at	2,47177225	2,27E-07
PCSK9	Pro protein convertase subtilisin/kexintype 9	11723499_a_at	2,46441396	9,53E-05

IL1RN	Interleukin 1 receptor antagonist	11740722_a_at	2,46216642	2,59E-10
		11719754_s_at	2,4316404	1,05E-10
C1R	Complement C1R	11742699_a_at	2,45823127	9,26E-03
		11742701_x_at	2,38889976	1,37E-02
ADAMTSL4	ADAMTS like 4	11755688_a_at	2,4534119	1,22E-03
		11748060_a_at	2,3614979	1,28E-03
CYP4F3	Cytochrome P450 family 4 subfamily F member 3	11759103_at	2,45306456	1,44E-02
		11733297_at	2,12183153	2,97E-02
		11749604_s_at	2,11727243	1,78E-03
		11749758_s_at	2,01384977	1,58E-03
LIPH	Lipase H	11727621_a_at	2,4441618	1,61E-05
MX1	MX dynamin like GTPase1	11716167_a_at	2,44325645	1,08E-03
IFIT3	Interferon induced protein with tetratrico peptide repeats 3	11731407_x_at	2,4383535	1,75E-09
DUSP10	Dual specificity phosphatase 10	11729169_a_at	2,42564527	4,29E-06
		11751237_a_at	2,39292798	1,23E-05
		11729170_x_at	2,26095708	1,33E-05
NECTIN4	Nectin cell adhesion molecule 4	11728764_a_at	2,42519201	1,77E-02

		11728765_a_at	2,22202559	1,99E-02
SP100	SP100 nuclear antigen	11759828_s_at	2,41990159	1,49E-08
HERC6	HECT and RLD domain containing E3 ubiquitin protein ligase family member6	11723128_a_at	2,4128617	1,99E-07
RHOV	Ras homolog family member V	11732436_at	2,40649314	1,01E-02
		11732437_at	2,1196392	3,95E-02
TP53I11	Tumor protein p53 inducible protein 11	11744505_x_at	2,40495672	2,77E-04
CLK1	CDC like kinase 1	11716325_a_at	2,39049772	3,89E-08
		11744828_a_at	2,37502138	2,57E-08
		11744827_a_at	2,15633579	6,28E-08
GAST	Gastrin	11730167_at	2,38998044	2,37E-08
MAX	MY Cassociated factor X	11762234_a_at	2,38971825	1,46E-05
LOC554223	Histocompatibility antigen-related	11759857_at	2,37872076	4,37E-09
STARD4	StAR related lipid transferdomain containing 4	11736424_a_at	2,37732856	4,91E-04
		11751806_a_at	2,05911682	4,29E-04
WDR33	WD repeat domain 33	11758867_at	2,37331694	5,61E-07
S100A8	S100 calcium binding protein A8	11753823_a_at	2,36601184	1,84E-03
TMEM40	Transmembrane protein 40	11745249_x_at	2,36083364	4,10E-08

SPTAN1	Spectrin alpha, non-erythrocytic 1	11760403_at	2,35152074	5,43E-03
ITGB7	Integrin subunit beta7	11725966_a_at	2,34773165	1,93E-06
HLA-F	Major histocompatibility complex, classI, F	11732355_x_at	2,34665721	1,29E-03
		11732354_a_at	2,28221989	1,78E-03
		11762112_a_at	2,22194896	5,03E-03
STAT2	Signal transducer and activator of transcription 2	11760880_a_at	2,31504166	3,85E-05
RDM1	RAD 52 motif containing 1	11742640_x_at	2,31177318	1,96E-06
		11742639_a_at	2,23184535	5,02E-07
RARRES3	Retinoic acid receptor responder 3	11719692_a_at	2,30853847	3,77E-04
		11748907_a_at	2,27141367	6,44E-04
HLA-DRB4	Major histocompatibility complex, classII, DR beta4	11755998_x_at	2,29741206	1,27E-05
EPB41L4A-AS1	EPB41L4A antisense RNA1	11744369_s_at	2,29263025	1,26E-09
CTSS	Cathepsin S	11749589_x_at	2,29254839	4,00E-04
SLC28A3	Solute carrier family 28 member 3	11746755_s_at	2,2879234	1,39E-02
		11738068_a_at	2,10897098	1,01E-02
IFIH1	Interferon induced with helicase C domain 1	11724346_a_at	2,28333614	7,38E-09
RAET1G	Retinoic acid early transcript 1G	11737483_at	2,28123961	1,74E-06

TXNIP	Thioredoxin interacting protein	11717190_s_at	2,27480428	2,82E-05
		11748544_s_at	2,01453907	6,00E-04
MAL	Mal,T-cell differentiation protein	11754728_a_at	2,26988687	3,53E-03
OSMR	Oncostatin M receptor	11759644_at	2,26919844	4,62E-04
DBP	D-box binding PAR b ZIP transcription factor	11731661_s_at	2,25395226	1,13E-05
		11752942_s_at	2,11825631	6,60E-06
MMP7	Matrix metallo peptidase 7	11744031_at	2,25020308	2,62E-02
HLA-DMB	Major histocompatibility complex, classII, DM beta	11746961_a_at	2,24740417	6,12E-07
		11754681_s_at	2,07195672	3,87E-07
SRSF5	Serine and arginine rich splicing factor 5	11760242_a_at	2,23566478	5,55E-08
NXNL2	Nucleoredoxin-like2	11715332_at	2,23114554	9,19E-06
		11715333_s_at	2,14713165	6,40E-07
CDKN2AIPNL	CDKN2A interacting protein N-terminal like	11762335_a_at	2,229171	1,08E-07
SLPI	Secretory leukocyte peptidase inhibitor	11716033_at	2,21510515	5,17E-03
SPRR2D	Small proline rich protein 2D	11729266_x_at	2,21436707	5,62E-07
		11729265_at	2,0095301	1,06E-07
IL32	Interleukin 32	11735174_a_at	2,21357442	1,10E-06

		11736394_x_at	2,07254921	1,45E-06
		11753515_a_at	2,00744935	1,09E-05
HLA-DMA	Major histocompatibility complex, classII, DM alpha	11716554_a_at	2,20997183	1,65E-05
		11745989_a_at	2,14663742	1,21E-05
IFI44	Interferon induced protein 44	11719886_a_at	2,20874269	1,29E-07
		11746088_a_at	2,11344233	9,69E-09
		11760254_at	2,02528941	1,27E-03
RPL22L1	Ribosomal protein L22 like 1	11733816_a_at	2,20835601	6,01E-07
SERPINB10	Serpin family B member 10	11732971_at	2,20092454	1,50E-02
SLC30A1	Solute carrier family 30 member 1	11726006_at	2,20068699	3,25E-06
CDKN2B	Cyclin dependent kinase inhibitor 2B	11736163_a_at	2,19406833	3,80E-05
TMPRSS11E	Transmembrane protease, serine 11E	11736715_s_at	2,19328052	1,19E-03
SNAPC3	Small nuclear RNA activating complex polypeptide 3	11739238_at	2,19257915	9,02E-07
H1F0	H1 histone family member 0	11718484_s_at	2,18976814	2,48E-04
SALL4	Spalt like transcription factor 4	11728065_a_at	2,18953409	1,20E-06
HRASLS2	HRAS like suppressor 2	11734396_at	2,18737415	2,06E-05
DAPK2	Death associated protein kinase 2	11730526_x_at	2,18681572	8,82E-03

		11730527_a_at	2,16504346	4,46E-03
		11748604_a_at	2,02108541	1,42E-03
HCP5	HLA complex P5 (non-proteincoding)	11720923_a_at	2,18646176	9,29E-06
		11720922_a_at	2,1731262	1,46E-05
SYNGR3	Synaptogyrin 3	11723055_a_at	2,18514384	5,81E-05
FRMD4B	FERM domain containing 4B	11731574_at	2,18149664	4,56E-04
ALPP	Alkaline phosphatase, placental	11723748_at	2,18098291	5,75E-10
		11752432_s_at	2,08080025	6,04E-08
IFIT2	Interferon induced protein with tetratricopeptide repeats 2	11721873_at	2,17666811	1,60E-08
		11721874_at	2,0397551	1,28E-08
KRT9	Keratin 9	11738533_a_at	2,17358688	1,19E-04
IRF7	Interferon regulatory factor 7	11718916_a_at	2,16093676	7,06E-05
DUSP5	Dual specificity phosphatase 5	11717863_a_at	2,15694455	3,17E-07
ZBTB43	Zinc finger and BTB domain containing 43	11722290_a_at	2,15481293	4,01E-09
SLC5A1	Solute carrier family 5 member 1	11736297_a_at	2,15262859	3,00E-03
N4BP2L1	NEDD4 binding protein 2 like 1	11732531_s_at	2,15021377	1,34E-03
JPH2	Juncto philin 2	11754657_a_at	2,14779358	2,31E-06

ISG15	ISG15 ubiquitin-like modifier	11716895_s_at	2,14747109	7,70E-06
RNF39	Ring finger protein 39	11731326_a_at	2,14166191	6,60E-04
FAXDC2	Fatty acid hydroxylase domain containing 2	11748570_a_at	2,14066022	4,76E-03
FLCN	Folliculin	11725448_at	2,13993736	1,52E-03
GPR37L1	G protein-coupled receptor 37 like 1	11734711_at	2,13987042	6,19E-09
FOXN1	Forkhead box N1	11741474_at	2,13536102	1,57E-07
CALCOCO1	Calcium binding and coiled-coil domain 1	11716080_a_at	2,13445068	1,69E-03
		11716079_a_at	2,04786581	6,19E-04
ACBD4	Acyl-Co A binding domain containing 4	11742135_at	2,13442369	1,28E-07
MARCKSL1	MARCKS like 1	11743722_x_at	2,13346045	6,08E-06
APOL1	Apolipoprotein L1	11735997_x_at	2,13254062	4,04E-06
SYT17	Synaptotagmin 17	11758988_at	2,12228248	1,71E-02
TMOD1	Tropomodulin 1	11732501_a_at	2,12167785	9,36E-05
CEACAM5	Carcino embryonic antigen related cell adhesion molecule 5	11739039_x_at	2,12152385	1,34E-06
WIPI1	WD repeat domain, phosphoinositide interacting 1	11747808_a_at	2,11962343	6,37E-08
		11717413_a_at	2,03372898	7,96E-07
FAM46B	Family with sequence similarity 46 member B	11726113_a_at	2,11952721	1,81E-03

ALPPL2	Alkaline phosphatase, placental like 2	11727334_at	2,11815984	4,26E-07
ICAM1	Intercellular adhesion molecule 1	11747499_a_at	2,11686119	1,04E-06
TIPARP	TCDD induciblepoly (ADP-ribose)polymerase	11755700_a_at	2,11068339	1,21E-08
HCAR2	Hydroxy carboxylic acid receptor 2	11722615_s_at	2,10595823	1,73E-04
C10orf54	Chromosome 10 open reading frame 54	11718001_a_at	2,10357154	9,04E-05
CYBRD1	Cytochrome B reductase 1	11716310_a_at	2,1034393	7,38E-09
RHCE	RH blood group CcEe antigens	11740680_s_at	2,10332929	3,60E-06
		11742143_s_at	2,05736019	1,43E-04
		11742315_s_at	2,02641635	2,77E-05
NATD1	N-acetyl transferase domain containing 1	11723885_at	2,10259655	6,91E-05
HLA-DRB5	Major histocompatibility complex, classII, DR beta5	11720657_x_at	2,10008694	1,94E-07
PLAU	Plasminogen activator, urokinase	11754119_a_at	2,09871101	7,39E-06
FA2H	Fatty acid2-hydroxylase	11724063_s_at	2,08922024	9,72E-08
GLRX	Glutaredoxin	11718049_s_at	2,08655525	8,28E-05
TMPRSS4	Transmembrane protease, serine 4	11721268_s_at	2,08277122	5,67E-07
IRF1	Interferon regulatory factor 1	11754035_a_at	2,08259472	3,44E-03
DGAT2	Diacylglycerol O-acyltransferase 2	11722642_a_at	2,08230163	3,72E-07

SLC15A3	Solute carrier family 15 member 3	11746309_a_at	2,08203049	1,91E-06
GCA	Grancalcin	11748497_s_at	2,07902366	7,73E-08
OVOL1	Ovo like transcriptional repressor 1	11725477_at	2,07782688	9,77E-08
FKBP1A-SDCBP2	FKBP1A-SDCBP2 read through (NMD candidate)	11718933_s_at	2,07749729	1,77E-03
YOD1	YOD1 deubiquitinase	11724635_at	2,0771578	1,38E-06
TRIM31	Tripartite motif containing 3	11728409_a_at	2,07480418	1,33E-02
NEU1	Neuraminidase 1	11715838_a_at	2,07404132	1,52E-08
IDI1	Isopentenyl-diphosphatedeltaisomerase1	11744474_s_at	2,07301916	4,21E-08
IL6	Interleukin 6	11746463_a_at	2,0725557	8,09E-07
FIP1L1	Factor interacting with PAPOLA and CPSF1	11759533_s_at	2,07077672	1,32E-07
PIM1	Pim-1 proto-oncogene, serine/threonine kinase	11717256_at	2,07016264	2,58E-05
FLVCR2	Feline leukemia virus subgroup C cellular receptor family member 2	11749946_a_at	2,06965274	2,57E-06
TMEM27	Transmembrane protein 27	11722244_at	2,06749083	1,41E-07
IL36RN	Interleukin 36 receptor antagonist	11732734_a_at	2,06242257	3,04E-07
ISG20	Interferon stimulated exonuclease gene 20	11756806_a_at	2,06014593	5,31E-10
MAFF	MAFbZIP transcription factor F	11726611_x_at	2,04898854	1,50E-05

AVPI1	Arginine vasopressin induced 1	11717678_at	2,04763777	1,42E-06
FAM63B	Family with sequence similarity 63 member B	11730885_a_at	2,04553573	3,58E-08
RAB18	RAB18, member RAS oncogene family	11759586_s_at	2,04137416	2,45E-03
STOM	Stomatin	11749252_a_at	2,04044523	1,45E-04
HSD17B2	Hydroxysteroid17-betadehydrogenase 2	11744099_a_at	2,03915973	7,41E-04
NMU	Neuromedin U	11728376_s_at	2,03856191	4,63E-05
FGF2	Fibroblast growth factor 2	11725039_at	2,0377119	8,49E-06
SLC2A14	Solute carrier family 2 member 14	11736555_s_at	2,03763604	8,25E-04
TEF	TEF, PARbZIP transcription factor	11724304_a_at	2,03520286	5,07E-08
KIF26A	Kinesin family member 26 A	11729429_a_at	2,02143331	6,50E-04
KRT23	Keratin 23	11744424_a_at	2,01643472	3,48E-08
PGLYRP4	Peptido glycan recognition protein 4	11732778_at	2,01037625	1,53E-02
PGBD5	Piggy Bac transposable element derived 5	11722327_at	2,00473376	9,18E-07
ABHD4	AB hydrolase domain containing 4	11718255_at	2,00380499	1,05E-05
ALDH3B1	Aldehydedehydrogenase 3 family member B1	11731722_a_at	2,00293975	8,65E-09

Genes subexpresados en el microarreglo

Gene symbol	Gene name	Probe	Fold Change	Adj. p.Val
DNAJB6	DNA J heat shock protein family (Hsp40) member B6	11716331_a_at	-5,406303515	2,25E-11
		11747937_a_at	-5,406303515	2,25E-11
EGLN3	Egl-9 family hypoxia inducible factor 3	11757444_a_at	-4,793098469	1,26E-09
		11733852_at	-2,488215655	9,23E-06
LCMT2	Leucine carboxyl methyltransferase 2	11758091_s_at	-3,605695487	7,50E-11
		11749566_s_at	-3,24501158	1,28E-09
SRSF1	Serine and arginine rich splicing factor 1	11747684_a_at	-3,563013514	3,54E-10
PPP1R10	Protein phosphatase 1 regulatory subunit 10	11718253_a_at	-3,44382023	6,71E-07
		11718254_a_at	-3,018503073	7,57E-07
CXCL1	C-X-C motif chemokine ligand 1	11719366_s_at	-3,315187624	5,69E-08
JUN	Jun proto-oncogene, AP-1 transcription factor subunit	11718397_s_at	-3,260159976	1,01E-06
STC1	Stanniocalcin 1	11724197_at	-3,216496807	8,19E-05
		11750279_a_at	-2,010016249	2,14E-03

THBS1	Thrombospondin 1	11758842_at	-3,208173944	7,82E-07
CBS	Cystathionine-beta-synthase	11744287_x_at	-3,063457775	8,19E-09
		11744285_a_at	-2,865324366	6,19E-09
		11744286_s_at	-2,841484096	5,64E-09
		11744835_s_at	-2,825520788	1,34E-09
		11752656_a_at	-2,819109624	2,59E-10
		11745019_a_at	-2,360179965	3,01E-10
TRIM66	Tripartite motif containing 66	11728016_at	-3,040560693	9,99E-04
		11728015_at	-2,207667061	2,22E-02
BCAT1	Branched chain amino acid transaminase 1	11749782_x_at	-3,040195421	1,77E-07
		11749895_a_at	-2,861703055	5,19E-08
		11749780_a_at	-2,758347264	1,35E-07
		11749781_s_at	-2,68107469	3,45E-08
		11720566_at	-2,588033523	8,77E-08
SAMD12	Sterile alpha motif domain containing 12	11727336_at	-3,016025553	9,39E-06
SRSF8	Serine and arginine rich splicing factor 8	11722351_at	-3,00182233	1,89E-09
FGFR1OP2	FGFR1 oncogene partner 2	11744747_a_at	-2,998841102	2,25E-11

		11744748_x_at	-2,4083746	6,93E-09
ELAC1	ElaC ribonuclease Z 1	11723518_at	-2,98788263	5,19E-10
ZNF658	Zinc finger protein 658	11731891_s_at	-2,964891621	1,22E-05
		11741856_s_at	-2,60139876	1,61E-05
EGR1	Early growth response 1	11717860_a_at	-2,962714706	2,72E-02
		11717861_a_at	-2,704328329	3,08E-02
		11717862_x_at	-2,684276899	3,61E-02
		11752940_a_at	-2,619531308	4,25E-02
		11751643_x_at	-2,404458519	4,20E-02
		11754334_s_at	-2,143223877	1,84E-02
MYO10	Myosin X	11742414_x_at	-2,913889714	7,06E-08
PACS2	Phosphofurin acidic cluster sorting protein 2	11727954_at	-2,88223827	1,90E-09
VANGL1	VANGL planar cell polarity protein 1	11724649_at	-2,87054387	1,76E-05
SFXN2	Sideroflexin 2	11756286_a_at	-2,85919536	5,06E-09
NT5DC2	5'-nucleotidase domain containing 2	11756412_a_at	-2,854822384	3,02E-07
CXCL8	C-X-C motif chemokine ligand 8	11718841_s_at	-2,842940996	2,29E-07
		11754026_a_at	-2,762149608	2,73E-06

		11763226_x_at	-2,241393193	7,25E-07
HOXA7	Homeobox A7	11732633_at	-2,813063462	2,71E-09
ARSB	Arylsulfatase B	11731767_at	-2,737869273	3,73E-06
HIST1H1A	Histone cluster 1 H1 family member a	11734465_at	-2,734383282	3,86E-07
CASK	Calcium/calmodulin dependent serine protein kinase	11721586_a_at	-2,722570349	3,89E-06
LNP1	Leukemia NUP98 fusion partner 1	11724001_a_at	-2,707926338	1,26E-06
FBN2	Fibrillin 2	11729243_s_at	-2,686036783	4,65E-07
		11729242_at	-2,200698832	2,83E-07
GJA1	Gap junction protein alpha 1	11716329_s_at	-2,679399137	6,56E-04
		11716328_a_at	-2,152830649	1,11E-03
ANKRD36	Ankyrin repeat domain 36	11759886_x_at	-2,677512111	7,27E-03
		11754694_a_at	-2,664401845	1,20E-02
GUCY1A3	Guanylate cyclase 1 soluble subunit alpha	11749919_a_at	-2,658849417	1,84E-05
RGS16	Regulator of G-protein signaling 16	11746705_a_at	-2,631556454	2,20E-03
		11720943_a_at	-2,070125966	1,69E-03
FMN1	Formin 1	11759344_at	-2,594166952	2,35E-06
SRSF3	Serine and arginine rich splicing factor 3	11757962_s_at	-2,573491553	3,03E-09

		11723039_x_at	-2,541991453	3,62E-09
PMEPA1	Prostate transmembrane protein, androgen induced 1	11716149_a_at	-2,557025166	1,30E-08
SPRY1	Sprouty RTK signaling antagonist 1	11717652_s_at	-2,555695244	1,75E-06
		11738073_s_at	-2,555695244	1,75E-06
PTHLH	Parathyroid hormone like hormone	11740245_a_at	-2,549322459	8,99E-04
		11731897_a_at	-2,373297399	4,53E-03
MXRA7	Matrix remodeling associated 7	11743645_s_at	-2,536260541	1,35E-07
TSEN2	tRNA splicing endonuclease subunit 2	11742936_a_at	-2,522961261	9,16E-07
ENTPD1	Ectonucleoside triphosphate diphosphohydrolase 1	11724008_a_at	-2,520944277	1,88E-06
TRERF1	Transcriptional regulating factor 1	11727642_a_at	-2,520191459	7,65E-06
		11727643_s_at	-2,096673123	6,80E-07
CASP14	Caspase 14	11715288_s_at	-2,515431606	5,70E-03
		11759142_at	-2,225160071	5,92E-03
NCOA5	Nuclear receptor coactivator 5	11749705_a_at	-2,500764695	1,44E-08
		11718004_a_at	-2,348407375	4,38E-08
SH3RF2	SH3 domain containing ring finger 2	11763206_at	-2,500734173	1,33E-05
		11763207_at	-2,497077329	1,15E-05

HMGB3	High mobility group box 3	11754183_s_at	-2,477933325	3,14E-04
HIST1H2AI	Histone cluster 1 H2A family member i	11759252_at	-2,466046103	8,91E-09
		11759253_x_at	-2,12473801	1,72E-08
		11715219_s_at	-2,090081807	2,45E-09
TNC	Tenascin C	11716063_at	-2,461969141	2,98E-04
		11752009_a_at	-2,418146829	9,69E-05
		11747935_a_at	-2,387801168	3,47E-05
		11716062_a_at	-2,178315216	5,79E-05
WDR33	WD repeat domain 33	11721494_at	-2,443823436	3,61E-07
		11721497_s_at	-2,163239262	4,01E-07
		11721495_a_at	-2,124144281	1,89E-08
CCT6B	Chaperonin containing TCP1 subunit 6B	11745585_a_at	-2,425784815	2,58E-04
MRTO4	MRT4 homolog, ribosome maturation factor	11724751_at	-2,421736901	6,87E-06
HAS2	Hyaluronan synthase 2	11749553_a_at	-2,400683724	3,14E-04
		11740311_at	-2,359075595	4,01E-04
		11740312_at	-2,082384482	8,81E-04
ENAH	Enabled homolog (Drosophila)	11722843_a_at	-2,398931564	1,58E-03

PCF11	PCF11 cleavage and polyadenylation factor subunit	11722295_at	-2,389021619	1,38E-05
		11755004_a_at	-2,214300215	1,65E-06
SETMAR	SET domain and mariner transposase fusion gene	11755343_s_at	-2,388048103	1,75E-08
NFYA	Nuclear transcription factor Y subunit alpha	11725735_a_at	-2,373266062	5,72E-07
SLC25A13	Solute carrier family 25 member 13	11743477_at	-2,365743327	2,47E-05
		11746815_a_at	-2,349738846	8,62E-05
		11743476_a_at	-2,100285101	1,36E-04
SLC19A1	Solute carrier family 19 member 1	11759443_at	-2,363764749	9,68E-07
		11746270_a_at	-2,13260665	6,24E-04
		11758257_s_at	-2,010689214	1,80E-05
UBASH3B	Ubiquitin associated and SH3 domain containing B	11727816_at	-2,360757754	3,07E-07
CERK	Ceramide kinase	11717115_at	-2,353358122	4,26E-07
USP9X	Ubiquitin specific peptidase 9, X-linked	11725330_a_at	-2,345353975	3,81E-06
FER	FER tyrosine kinase	11763327_at	-2,3394786	1,34E-06
		11763325_a_at	-2,11834967	4,31E-06
		11763326_s_at	-2,036067449	1,26E-06
MYO5C	Myosin VC	11745120_a_at	-2,336055914	3,48E-08

PLEKHA8	Pleckstrin homology domain containing A8	11760553_a_at	-2,334836245	7,73E-08
ACTR3B	ARP3 actin related protein 3 homolog B	11737056_a_at	-2,330358616	3,48E-08
TTC12	Tetratricopeptide repeat domain 12	11755376_a_at	-2,326091206	7,90E-10
KMT5B	Lysine methyltransferase 5B	11739403_at	-2,323294115	1,69E-04
HDAC4	Histone deacetylase 4	11743453_s_at	-2,308295865	3,25E-07
MTDH	Metadherin	11757718_a_at	-2,303003742	1,03E-06
BMPR2	Bone morphogenetic protein receptor type 2	11756105_a_at	-2,297894762	5,38E-04
HYAL1	Hyaluronoglucosaminidase 1	11740989_a_at	-2,296066569	7,57E-04
		11740990_x_at	-2,262294971	5,75E-04
RBM15B	RNA binding motif protein 15B	11717684_at	-2,296057091	1,38E-09
CALB2	Calbindin 2	11725082_a_at	-2,288269161	1,80E-02
KRCC1	Lysine rich coiled-coil 1	11726003_a_at	-2,287612022	1,54E-05
VAPB	VAMP associated protein B and C	11758066_s_at	-2,279166424	1,73E-06
		11717584_a_at	-2,128027894	4,42E-08
TCF4	Transcription factor 4	11724239_at	-2,276357503	3,89E-07
ABCD3	ATP binding cassette subfamily D member 3	11741591_at	-2,269754535	1,35E-08
HOMER1	Homer scaffolding protein 1	11725386_a_at	-2,260988482	1,80E-04

		11725387_x_at	-2,145118512	1,09E-04
DHFR	Dihydrofolate reductase	11747280_x_at	-2,256988511	2,96E-07
ANP32A	Acidic nuclear phosphoprotein 32 family member A	11739079_a_at	-2,247330289	1,38E-10
GMPPB	GDP-mannose pyrophosphorylase B	11744100_a_at	-2,2471495	2,85E-08
ALG14	ALG14, UDP-N-acetylglucosaminyltransferase subunit	11743909_at	-2,242614519	1,72E-08
OSMR	Oncostatin M receptor	11733184_a_at	-2,23690231	2,65E-05
		11733185_at	-2,016915194	7,49E-05
FST	Follistatin	11732713_at	-2,22738175	9,69E-09
PDSS2	Prenyl (decaprenyl) diphosphate synthase, subunit 2	11748697_a_at	-2,218001648	1,66E-08
RPS23	Ribosomal protein S23	11719784_x_at	-2,215019166	2,92E-07
SCFD2	Sec1 family domain containing 2	11723959_at	-2,207168306	6,82E-07
		11723960_at	-2,090720165	8,14E-06
SYNCRIP	Synaptotagmin binding cytoplasmic RNA interacting protein	11720666_at	-2,207065299	4,03E-08
		11752628_a_at	-2,052013298	5,14E-08
HIST2H2AB	Histone cluster 2 H2A family member b	11759284_at	-2,204785504	1,10E-08
		11715148_s_at	-2,024460729	1,44E-08
IPO4	Importin 4	11719170_a_at	-2,20421333	9,74E-05

DPH3	Diphthamide biosynthesis 3	11733040_a_at	-2,185069852	1,34E-07
CNTF	Ciliary neurotrophic factor	11734208_s_at	-2,184660854	1,48E-05
FUCA1	Fucosidase, alpha-L- 1, tissue	11757005_a_at	-2,181963277	1,93E-06
BEND3	BEN domain containing 3	11725579_s_at	-2,180979935	8,54E-06
		11725578_at	-2,085562679	6,64E-05
CALM1	Calmodulin 1	11724759_s_at	-2,178135293	2,26E-06
DDX39A	DExD-box helicase 39A	11747334_a_at	-2,17792202	6,61E-07
UBA52	Ubiquitin A-52 residue ribosomal protein fusion product 1	11729104_x_at	-2,176489808	2,06E-10
STEAP1B	STEAP family member 1B	11757071_s_at	-2,173708417	1,73E-04
VARS	Valyl-tRNA synthetase	11743987_a_at	-2,171952752	2,15E-05
		11743988_x_at	-2,14133321	1,04E-05
TAF6L	TATA-box binding protein associated factor 6 like	11747503_a_at	-2,171900738	4,65E-07
FOXP1	Forkhead box P1	11758236_s_at	-2,171634885	2,73E-04
NPIPA5	Nuclear pore complex interacting protein family member A5	11759716_x_at	-2,155326292	1,57E-08
CSTF3	Cleavage stimulation factor subunit 3	11717642_a_at	-2,153454902	1,89E-09
PRKDC	Protein kinase, DNA-activated, catalytic polypeptide	11719391_a_at	-2,152625042	1,68E-08
		11740423_a_at	-2,050104356	4,78E-09

HEATR3	HEAT repeat containing 3	11740109_a_at	-2,151783006	4,76E-07
TFRC	Transferrin receptor	11715478_a_at	-2,145972536	2,29E-04
		11715477_at	-2,002406004	1,10E-04
TNRC6B	Trinucleotide repeat containing 6B	11758580_s_at	-2,145330815	3,24E-05
		11740670_a_at	-2,02976061	2,17E-06
GCFC2	GC-rich sequence DNA-binding factor 2	11739789_a_at	-2,143257214	1,84E-08
SERHL2	Serine hydrolase-like 2	11762076_at	-2,140637824	4,43E-08
DFFB	DNA fragmentation factor subunit beta	11745693_a_at	-2,137091816	1,38E-07
HIST1H2BE	Histone cluster 1 H2B family member e	11759168_x_at	-2,130917929	1,02E-05
ATP6V1E2	ATPase H+ transporting V1 subunit E2	11728554_at	-2,130666097	4,41E-05
GSPT1	G1 to S phase transition 1	11718222_s_at	-2,130495117	2,28E-06
		11718221_a_at	-2,026485654	1,68E-06
TPCN1	Two pore segment channel 1	11747544_a_at	-2,128406866	2,37E-08
NABP1	Nucleic acid binding protein 1	11763367_at	-2,124414402	1,88E-02
		11726727_a_at	-2,030736288	5,29E-08
STEAP1	STEAP family member 1	11725158_at	-2,12247975	1,19E-03
PSPH	Phosphoserine phosphatase	11754138_s_at	-2,113566277	1,33E-06

TIGAR	TP53 induced glycolysis regulatory phosphatase	11719731_at	-2,112734686	1,75E-07
MUM1	Melanoma associated antigen (mutated) 1	11721395_a_at	-2,110373778	1,54E-08
CD70	CD70 molecule	11761421_at	-2,108356377	1,65E-02
RPL27A	Ribosomal protein L27a	11736810_at	-2,106114644	5,43E-03
PLXNA2	Plexin A2	11720563_at	-2,105070072	3,83E-07
SFPQ	Splicing factor proline and glutamine rich	11720474_a_at	-2,097010279	5,92E-09
		11720475_x_at	-2,060313952	3,12E-09
RABGAP1L	RAB GTPase activating protein 1 like	11724325_a_at	-2,094252726	1,58E-05
WDR4	WD repeat domain 4	11739322_a_at	-2,091122835	4,39E-07
SLC11A2	Solute carrier family 11 member 2	11759691_a_at	-2,086769346	7,72E-07
C2orf68	Chromosome 2 open reading frame 68	11718384_at	-2,085406373	1,29E-04
HNRNPM	Heterogeneous nuclear ribonucleoprotein M	200072_PM_s_at	-2,079029392	7,49E-08
ILF3	Interleukin enhancer binding factor 3	11740781_a_at	-2,077792127	4,58E-09
		11718546_s_at	-2,016408044	2,25E-07
NRG1	Neuregulin 1	11755968_a_at	-2,077294058	3,22E-05
ADCK1	aarF domain containing kinase 1	11737704_s_at	-2,074382253	3,45E-06
FLG	Filaggrin	11741116_at	-2,070811964	4,72E-02

ADAMTS12	ADAM metallopeptidase with thrombospondin type 1 motif 12	11741341_a_at	-2,069687192	8,56E-10
DFFA	DNA fragmentation factor subunit alpha	11726261_at	-2,068865312	3,26E-07
CPSF6	Cleavage and polyadenylation specific factor 6	11744958_x_at	-2,065738686	4,74E-09
KCNAB1	Potassium voltage-gated channel subfamily A member regulatory beta subunit 1	11741274_a_at	-2,06186939	1,20E-04
PSAT1	Phosphoserine aminotransferase 1	11751230_a_at	-2,061325292	6,36E-04
NCS1	Neuronal calcium sensor 1	11720399_s_at	-2,059838466	2,75E-07
USP13	Ubiquitin specific peptidase 13 (isopeptidase T-3)	11722911_at	-2,059077154	9,03E-06
HIST1H1B	Histone cluster 1 H1 family member b	11738438_at	-2,057145735	6,47E-08
FDXACB1	Ferredoxin-fold anticodon binding domain containing 1	11746285_a_at	-2,054751557	2,56E-05
RFLNB	Refilin B	11724993_at	-2,053812646	2,77E-07
SGK1	Serum/glucocorticoid regulated kinase 1	11715931_s_at	-2,051618043	4,95E-02
MARS2	Methionyl-tRNA synthetase 2, mitochondrial	11729710_a_at	-2,050239604	7,25E-04
HIST2H3C	Histone cluster 2 H3 family member c	11742410_s_at	-2,046210186	7,37E-07
ANAPC7	Anaphase promoting complex subunit 7	11735948_a_at	-2,041279235	1,46E-07
CTBP1-AS2	CTBP1 antisense RNA 2 (head to head)	11740391_x_at	-2,040979621	2,11E-06
PSKH1	Protein serine kinase H1	11721725_at	-2,037699797	7,32E-08
MRRF	Mitochondrial ribosome recycling factor	11747410_a_at	-2,037157636	4,56E-09

SHROOM2	Shroom family member 2	11727274_a_at	-2,034194636	6,20E-08
CDK6	Cyclin dependent kinase 6	11723244_at	-2,032459476	2,49E-09
MDN1	Midasin AAA ATPase 1	11759195_a_at	-2,032270872	1,72E-07
ALDH1B1	Aldehyde dehydrogenase 1 family member B1	11746588_a_at	-2,028787064	2,69E-04
HIST1H3A	Histone cluster 1 H3 family member a	11715121_s_at	-2,027262978	3,80E-07
RAB3IP	RAB3A interacting protein	11758481_s_at	-2,023466343	2,87E-04
CAD	Carbamoyl-phosphate synthetase 2, aspartate transcarbamylase, and dihydroorotase	11718531_a_at	-2,018474644	5,87E-05
SEPHS1	Selenophosphate synthetase 1	11763313_at	-2,017649847	2,06E-10
C1orf131	Chromosome 1 open reading frame 131	11749341_a_at	-2,013150565	6,65E-08
DDX31	DEAD-box helicase 31	11737700_a_at	-2,009816053	1,14E-07
RRP15	Ribosomal RNA processing 15 homolog	11733904_at	-2,009767428	1,20E-05
UVSSA	UV stimulated scaffold protein A	11756484_a_at	-2,009054911	4,72E-05
HSPA4	Heat shock protein family A (Hsp70) member 4	11758770_at	-2,004484067	1,45E-07
ST20-AS1	ST20 antisense RNA 1	11735074_at	-2,001149437	5,68E-07